FUTURE CLIMATE SCENARIOS FOR CALIFORNIA: FREEZING ISOCLINES, NOVEL CLIMATES, AND CLIMATIC RESILIENCE OF CALIFORNIA'S PROTECTED AREAS

A White Paper from the California Energy Commission's California Climate Change Center

Prepared for: California Energy Commission

Prepared by: University of California, Berkeley

JULY 2012

CEC-500-2012-022

David Ackerly

University of California, Berkeley

ACKNOWLEDGEMENTS

I thank J. Johnstone for assistance accessing daily climate records, and S. Veloz, R. Shaw, S. Weiss, and S. Loarie for discussions that greatly improved this manuscript. The Department of Botany, University of Cape Town, South Africa, kindly provided sabbatical hospitality while this paper was being written.

ABSTRACT

Twenty-first century climate change threatens biodiversity, ecosystem services, and human welfare. The diversity of responses and climate sensitivity among species and ecosystems presents a challenge for forecasting, conservation, and resource management. This paper explores several biotically informed analyses of current climates and future climate projections for California, and their implications for biological conservation. Section 1 examines shifts in the distribution of freezing events, mapping areas that are no longer projected to experience freeze events of various magnitudes by the end of the twenty-first century; whereas, they have experienced freezes in the past. These areas may be sensitive to vegetation shifts, as plants that are not cold tolerant expand their ranges northward and to higher elevations. Section 2 examines expanding, novel, shrinking, and disappearing climates of California, based on the areal extent occupied by different combinations of climatic conditions. Under more severe climate change scenarios, large areas of the desert and Central Valley regions may experience expanding and novel climates, while conditions along the coast and in the High Sierra are forecast to shrink in extent, and in some cases disappear. Such analyses provide a general framework for forecasting impacts of climate change on species and vegetation types that occupy these regions. Section 3 examines the climatic heterogeneity of California's protected area network, encompassing State and National Parks, National Forests, and other public and private conservation lands. Climatic heterogeneity is expected to enhance conservation in the twenty-first, promoting diversity of species that tolerate different conditions and allowing for dispersal along climate gradients in response to climate change. Large reserves, especially those spanning broad elevational gradients, are critical to encompass a broad range of present and future climates. These results highlight the value of large, connected areas for conservation in the face of climate change.

Keywords: isoclines, novel climates, isoclimates, topographic heterogeneity, resilience

Please use the following citation for this paper:

Ackerly, David D. 2012. ***Future Climate Scenarios for California: Freezing Isoclines, Novel Climates, and Climatic Resilience of California's Protected Areas.*** California Energy Commission. Publication number: CEC-500-2012-022.

TABLE OF CONTENTS

Acknowledgements ..... **i**

ABSTRACT ..... **ii**

TABLE OF CONTENTS ..... **iii**

LIST OF FIGURES ..... **iii**

LIST OF TABLES ..... **vi**

Introduction **1**

Section 1: Changes in the Distribution of Freezing Events under Future Climates **5**

Methods 6

Results 13

Discussion 17

Section 2: Mapping Disappearing and Novel Climates under Future Climate Scenarios **19**

Methods 23

Results 26

Discussion 32

Section 3: Topographic Heterogeneity and the Resilience of California's Protected Areas **34**

Methods 35

Results 39

Discussion 45

Conclusions **47**

References **49**

Glossary **53**

Appendix

LIST OF FIGURES

Figure 1. Ecoregions of California, Nevada and Surrounding Areas, from Olson et al. (2001). Black rectangle shows the spatial domain of the 2008 California Climate Change Impacts Assessment 4

Figure 2. Mean Monthly T_{min} for the Coldest Month in the 1971–2000 Historical Period, from the PRISM Interpolated Climate Surfaces. Solid dots show the position of climate stations in the U.S. Historical Climate Network. B. Minimum daily T_{min} for the corresponding month in panel A, calculated from Equation 1.1. 7

Figure 3. Plot of Minimum vs. Mean Daily T_{min} ($T_{min\text{-}min}$ vs. $T_{min\text{-}mean}$) for All Monthly Data from Western States in the U.S. Historical Climate Network (N = 209,134). The red line shows the best fit quadratic regression (see Equation 1.1). 9

Figure 4. Plot of the Proportion of Days per Month in which $T_{min} < T_{crit}$, vs. Mean Monthly T_{min}. Tcrit = 0°C (black points), -5°C (green points), or -10°C (blue points). For clarity, only N = 20000 points are shown, drawn randomly from the full data set. 11

Figure 5. Number of Months per Year (Averaged over 1971–2000) in which Monthly T_{min} Values Fall below Various Critical Levels. a, b: 0°C; c, d: -5°C; e, f: -10°C. a, c, e: Mean monthly T_{min}; b, d, f: Minimum monthly T_{min}. 15

Figure 6: Changes in the Distribution of Freeze Events Occurring at Least Once per 30 Years, from the 1971–2000 Historical Period to the 2071–2100 Future Projections, for the CCSM3 GCM. a, b, d: B1 emissions scenario; c, e, f: A2 emissions scenario. a,b: Freezing events less than critical temperature (T_{crit}) = 0 °C; c,d: T_{crit} < -5 °C; e,f: T_{crit} < -10 °C. Blue areas have experienced a freeze less than the indicated T_{crit} values in the past, and are projected to continue to experience these events in the future. Red areas have experienced these in the past, but are not projected to experience these in the future. Gray are areas that have not experienced a freeze at this temperature in the past, and will not in the future either. 16

Figure 7. Same as Figure 6, for Freezes Occurring on Average One or More Times per Year 17

Figure 8. Magnitude of Climate Change for California and Nevada, Measured as the Standardized Euclidean Distance between Historical (1971–2000) and Future (2070–2099) Conditions, Scaled by Historical Variability. Values > 5 (orange to red) generally represent future conditions beyond the range of historical variability (see text). 27

Figure 9. Example of an Expanding and a Shrinking Climate Type, from the CCSM3 A2 Scenario. The two conditions selected for illustration are outlined in black boxes in Table 1. a: Historical period, 1971–2000. b: Future period, 2070–2099. Orange: precipitation (mm, log) 2.43–3.03, Tmin (°C) -12.8 to -6.3 °C, Tmax (°C) 31.5–35.4, which expands from 8 pixels in the historical period to 127 pixels in the future. Blue: precipitation 1.84–2.43, Tmin 0.11–6.55, Tmax 35.4–39.3, which shrinks from 210 pixels to 92 pixels. 28

Figure 10. Novel, Disappearing, Expanding, and Shrinking Climates of California, for B1 Emissions Scenario. In each figure, left column shows fate of current climates (1971–2000); right column shows status of projected future climates (2071–2100). Rows represent results for the CNRM, GFDL, PCM1, and CCSM3 general circulation models, downscaled for the 2008 California Climate Change Impacts Assessment Report. Colors: black = disappearing; dark blue = >10-fold reduction; light blue = 1- to 10-fold reduction; yellow = 1- to 10-fold expansion; orange = >10-fold expansion; red = novel climate. For example, in a row, the areas mapped in

yellow on left contain climates that will expand up to 10-fold in area, occupying the areas shown in yellow on the right. 30

Figure 11. Same as Figure 10, for A2 Emissions Scenario 31

Figure 12. Conservation Units Derived from the California Protected Areas Database v.1.6. Units Were Defined as Contiguous Areas of > 1000 ha (see text for details). Gray scale is arbitrary, to highlight boundaries between adjacent reserves. 36

Figure 13. Eight Climate and Topographic Layers Used for Overlay on Conservation Units Database. Mean, standard deviation, and range for each parameter were calculated for each conservation unit. T_{min}: mean monthly minimum temperature; T_{max}: mean monthly maximum temperature; T_{mean}: mean annual temperature; T_{seas}: temperature seasonality, measured as standard deviation of monthly temperatures; P_{Ltot}: total annual precipitation (mm, log10 transformed); P_{seas}: precipitation seasonality, measured as coefficient of variation of monthly precipitation. 38

Figure 14. Elevational Range vs. Area for 623 Conservation Units Shown in Figure 3.1. See the text for a discussion of thresholds at the 1000 m elevation range, and 5000 and 50,000 ha area. A transparent color was used to highlight the large number of overlapping points in the lower left quadrant. 40

Figure 15. The Range of Environmental Conditions in Conservation Units, Relative to their Size and Elevational Range 42

Figure 16. Climate Overlap of Conservation Units, Relative to their Size, Elevational Range, and Minimum Distance to the Ocean. Left panels: pairwise scatterplots. Right panels: residuals of climate overlap after accounting for the other two factors. 45

Figure 17. Conservation Units Used in this Analysis; Areas with an Elevational Range of > 1000 m Are Outlined in Red. The blue box shows the size of 150,000 acres (= 61,000 ha), the minimum size for Landscape Reserves proposed in the 2009 California Climate Change Adaptation Strategy. 46

Figure A1. Distribution of Monthly T_{min} Data from the U.S. Historical Climate Network for Stations in the Western States. A: Number of monthly data sets available, by year. B: Time span covered by each station. Each horizontal line represents one station, sorted from bottom to top by start and end dates. Blue dots indicate months with available data. 54

Figure A2. Scatterplot of the Minimum Mean Monthly Temperature for the 1971–2000 Period from PRISM (x-axis) vs. the 2008 California Climate Change Impacts Assessment (CA2008) Downscaled GCM Outputs, for the Same Period. Red lines indicate x = y. Headers on each panel indicate the GCM and emissions scenario used. 55

Figure A3. Maps of Deviations in Minimum Mean Monthly Temperature between PRISM and CA2008 Scenarios, as Shown in Figure 1.6. Negative values indicate CA2008 temperatures are colder than the PRISM temperatures. 56

Figures A4–9. Changes in the Distribution of Freeze Events from the 1971–2000 Historical Period to the 2071–2100 Future Projections. Each map corresponds to a different future climate

scenario from the CA2008 downscaled projections, with the GCM and emissions scenario noted above. Dark lines show ecoregions (see Figure 2). Blue areas have experienced a freeze < the indicated T_{crit} values in the past, and are projected to continue to experience these events in the future. Red areas have experienced these in the past, but are not projected to experience these in the future. Green are areas that have not experienced a freeze at this temperature in the past, and will not in the future either. A4: T_{crit} < 0°C experienced at least once in the 30-year period. A5: T_{crit} < 0°C experienced at least once per year, on average, during the 30-year period. A6: T_{crit} < -5°C experienced at least once in the 30-year period. A7: T_{crit} < -5°C experienced at least once per year, on average, during the 30-year period. A8: T_{crit} < -10°C experienced at least once in the 30-year period. A9: T_{crit} < -10°C experienced at least once per year, on average, during the 30-year period. 57

Figure A5. T_{crit} < 0°C Experienced at Least Once per Year, on Average, during the 30-year Period (see the full description above) 58

Figure A6. T_{crit} < -5°C Experienced at Least Once in the 30-year Period (see the full description above) 59

Figure A7. T_{crit} < -5°C Experienced at Least Once per Year, on Average, during the 30-year Period (see the full description above) 60

Figure A8. T_{crit} < -10°C Experienced at Least Once in the 30-year Period (see the full description above) 61

Figure A9. T_{crit} < -10°C Experienced at Least Once per Year, on Average, during the 30-year Period (see the full description above) 62

Figure A10. Novel, Disappearing, Expanding, and Shrinking Climates of California, Nevada, and Surrounding Areas, for the B1 Emissions Scenario. In each figure, left column shows the fate of current climates (1971–2000); right column shows status of projected future climates (2071–2100). Rows represent results for the CNRM, GFDL, PCM1, and CCSM3 general circulation models, downscaled for the 2008 California Climate Change Impacts Assessment Report. Colors: black = disappearing; dark blue = >10-fold reduction; light blue = 1- to 10-fold reduction; yellow = 1- to 10-fold expansion; orange = >10-fold expansion; red = novel climate. For example, in a row, the areas mapped in yellow on left contain climates which will expand up to 10-fold in area, occupying the areas shown in yellow on the right. 63

Figure A11. Same as Figure A10, for A2 Emissions Scenario 64

LIST OF TABLES

Table 1. Abbreviations Used for Minimum Temperature Analysis 8

Table 2. Three-dimensional Histogram for Areas Occupied under Historical (left) and Future (right) Climates for the California State Domain (future in this example if CCSM3, A2, 2070–2099). The four subtables represent different precipitation levels (left column) and within each subtable, rows represent bins of maximum temperature and columns are bins of minimum

temperature (row and column labels show lower cutoffs for each bin). Values are the number of pixels occupied by each combination of climate values, where pixel size is 7.5 arc min, approximately 12 km on a side. Cells colors show fate of each climate, comparing historical and future values (and correspond to colors in Figures 10 and 11): gray = disappearing climate; dark blue = >10-fold reduction in area; light blue = 10- to 1-fold reduction; yellow = 1- to 10-fold expansion; orange = >10-fold expansion; red = novel climate. 25

All tables and figures are provided by the authors.

Introduction

Rapid climate change in the twenty-first century threatens biodiversity, ecosystem services, and human welfare. While climate change per se is a pervasive feature of earth history, the pace of change currently forecast for the next 100 years is virtually unparalleled in its speed, magnitude, and global extent (Barnosky 2009; see Willis et al. 2010). If the rate of change exceeds the pace of biological response, especially the capacity of populations to migrate or undergo adaptive evolutionary change, impacts on species distributions, community structure, and ecosystem function may be profound. Projecting the magnitude and distribution of these impacts poses a considerable challenge, requiring integration of theory and observation from a range of disciplines, including paleoecology, ecophysiology, population biology, and biogeography.

While rapid advances have been made in this regard, numerous uncertainties remain. One of the central challenges in understanding impacts on biodiversity is diversity itself, whether measured in terms of genotypes, species, or ecological communities. Ecological and evolutionary research has documented that species exhibit distinct responses to abiotic conditions and interactions with other taxa. An understanding of the vulnerability of individual species or ecosystems to climate change requires the synthesis of specific understanding of individual systems with general principles of conservation biology (Williams et al. 2008; Glick et al. 2011; Klausmeyer et al. 2011). While these analyses are critically important, it will not be possible to conduct detailed studies on more than a handful of species or ecosystems.

The vulnerability of natural and human systems to climate change can be considered a function of three components (Füssel and Klein 2006; Williams et al. 2008):

1. *Exposure*: Which components of climate are changing? What is the magnitude of the changes projected? And how fast will they occur?
2. *Sensitivity*: What is the intrinsic sensitivity of the system (i.e., population, species, ecosystem) to change, based on underlying physiological and ecological functioning?
3. *Adaptive Capacity*: What are the mechanisms and potential for the system to adapt to these changes and mitigate the impacts? In other words, what changes could occur that will reduce exposure or sensitivity over time, and what are the ecological and evolutionary processes that will promote such changes?

For plants, animals, and the ecosystems they inhabit, these three components are influenced both by human actions and features of the natural world. Exposure is primarily driven by the rate of climate change, which varies in different parts of the world due to the nature of the global climate system. Climate change mitigation efforts aim to reduce exposure, primarily via reduced greenhouse gas emissions, and provide the only direct and globally effective strategy to minimize climate change impacts. Sensitivity (of natural systems) is primarily a function of organismal physiology, population biology, and ecological functioning (e.g., thermal tolerances, reproductive rates, ecological interactions); at a landscape scale, environmental heterogeneity, dispersal barriers, and habitat loss will influence sensitivity as well. Adaptive capacity may arise from individual plasticity, evolutionary adaptation, or dispersal ability, allowing organisms to

adapt and move across the landscape as climate changes. Climate change adaptation strategies consist of conservation and management activities that can reduce sensitivity or facilitate adaptive responses (e.g., reserve acquisition, corridors) and minimize the eventual impacts of changing conditions.

Several recent studies have examined aspects of climate change and the existing conservation lands network to address general aspects of the vulnerability framework above in a spatial framework, independent of the particular species or communities involved. Williams et al. (2007) quantified the magnitude of projected climate change across the globe relative to historical climate variability, on the assumption that ecological systems will experience greater impacts if future climates exceed the historical range of variability. They also mapped the distribution of *novel* climates, i.e., climatic regimes projected for the future that are not observed now (either regionally or globally), and *disappearing* climates, regimes that occur in the present but are not observed under future scenarios. Understanding the nature and distribution of novel climate regimes is critical, as we do not have analogs in current ecosystems that can be used to project ecological responses to such conditions. Ackerly et al. (2010) and Wiens et al. (2011) also conducted analyses of disappearing and novel climates, using different approaches (see further discussion below).

Loarie et al. (2009) introduced the concept of the *velocity* of climate change, based on the speed at which climatic isoclines are projected to move across landscapes. Climate velocity is calculated as the ratio of the rate of projected climate change (e.g., °C/year) divided by the spatial gradient of climate at each point on the landscape (°C/kilometer [km]), resulting in a measure of velocity (km/yr). For temperature, rates of temporal change in California, under an ensemble of twenty-first climate scenarios, vary from 0.04–0.06°C/year. Spatial gradients, on the other hand, vary enormously due to topography, from less than 0.01°C/km in flat areas such as the Central Valley to as high as 5°C/km in mountainous terrain. As a result, the velocity of climate change can vary from less than 0.01 km/yr in mountains to almost 10 km/yr in flat areas (see Figure 1 in Loarie et al. 2009 and Figure 5 in Ackerly et al., 2012; Burrows et al. 2011 compare velocities in marine versus terrestrial ecosystems). This wide range emphasizes the critical influence of topography on biotic responses to climate change. In mountainous terrain, dispersal distances required for species to move and track changing climates are much shorter, and microclimate variation on small-scale topographic gradients makes them shorter still (Luoto and Heikkinen 2008; Randin et al. 2009; Ackerly et al. 2010; Scherrer and Körner 2011). Based on these velocities, there will be little or no overlap between present and future climates in most of the world's protected areas, except for the largest reserves and those in highly varied terrain (Araujo et al. 2004; Loarie et al. 2009; Ackerly et al. 2010).

Klausmeyer et al. (2011), focusing on California as a model system, brought together several approaches to produce an integrated measure of climate change impacts and implications for conservation at a regional scale. They quantified: *climate stress* as the magnitude of projected changes relative to historical variability (using a different algorithm than Williams et al. 2007); *landscape exposure*, based on topographic diversity, connectivity and distribution of water

sources; and *adaptive constraints*, based on habitat loss and fragmentation. From the various combinations of low and high levels for each of these features, they then discuss implications for regional conservation strategies, ranging from pursuit of current strategies (when all three factors are low) to a reassessment of conservation goals (when all are high).

These studies illustrate various approaches to the analysis of spatial and temporal patterns in historical and future climate data that can inform conservation planning, without reference to specific taxa or ecosystems. This paper builds on such analyses to assess the pattern and magnitude of climate change in California, based on projections from the 2008 California Climate Impacts Assessment, and the climatic diversity of the conservation lands network. The overall objective is to examine existing climate change projections from perspectives with well-defined biological and conservation implications. Section 1 examines spatial shifts in the distribution of freezing events, one aspect of climate that is known to have important impacts on ecological systems. Section 2 presents an analysis of novel and disappearing climates (following Ackerly et al. 2010) for California and surrounding areas, under a range of future scenarios. Section 3 examines the current climatic diversity of the existing conservation lands network, and the climatic overlap between historical and future climates within individual reserves in California (building on a similar analysis for the San Francisco Bay Area in Ackerly et al. 2010). Figure 1 illustrates ecoregions of the Western United States and the spatial domain of the 2008 California Climate Impacts Assessment. All analyses in this paper were conducted on publicly available data sets using spatial libraries and statistical tools in the open source and free R programming language (R Development Core Team 2006). Analysis scripts are available at: tinyurl.com/CECscripts.

Figure 1. Ecoregions of California, Nevada and Surrounding Areas, from Olson et al. (2001). Black rectangle shows the spatial domain of the 2008 California Climate Change Impacts Assessment.

Section 1: Changes in the Distribution of Freezing Events under Future Climates

Cold temperatures have an important influence on the distribution of individual species of plants and animals, as well as on major habitats and vegetation types (Woodward 1987). While many plants avoid cold by dropping leaves or remaining dormant below ground, woody evergreens continue to function through both cold and dry unfavorable seasons. Extreme cold can impact plant function in two main ways, either by damage to living tissues or by causing embolisms (air bubbles) in the water-conducting xylem elements (Sperry and Sullivan 1992; Davis et al. 1999; Stuart 2007]). The minimum temperature a plant can experience depends both on the extent of evolutionary adaptation to cold, as well as short-term acclimation responses. Exposure to cold induces "cold-hardening," increasing resistance to subsequent cold events. As a result, plant sensitivity to cold depends on both long-term historical climate, shaping evolutionary adaptation, and short-term weather events, influencing acclimation. As plants adapt to the "normal" range of historical climates, extreme cold events can have strong effects almost anywhere in the globe. For example, some chaparral shrubs in southern California demonstrate an unexpectedly high degree of sensitivity to unusual cold events, leading to leaf death and shoot dieback (Davis et al. 1999; Davis et al. 2007). Cold also has strong effects on many crops, and can limit the growing areas for tropical and subtropical crops such as citrus and avocado.

Several measures are available to translate climatic data and projections of future change to biologically relevant parameters. Growing-degree days (cumulative degrees above a threshold, summed over a season) are widely used in horticulture and agriculture, and can provide informative estimates of temperature effects on plant growth. Crops such as stone fruits (peaches and plums) have a winter chilling requirement, so climate warming presents a threat due to insufficient cold temperatures (see Luedeling et al. 2009). This study focuses on changes in the distribution of freezing events of varying severity, as plant and animal species differ in their minimum temperature tolerances. The distribution of frosts is particularly interesting in regions such as California where the strong marine influence results in infrequent frosts in coastal areas, and the expansion of the frost free zone raises the potential for qualitative shifts in vegetation and agriculture under future climate scenarios.

Understanding the role of cold, and forecasting future distribution of cold events, is difficult using standard climate data, which report mean monthly temperatures. This study's objective is to determine the relationship between mean monthly temperature and the frequency and intensity of freezing events, in order to develop transfer functions for use in geographic information systems (GIS), and in association with future climate projections. The frequency and distribution of freezing events (and other climate extremes) can also be obtained from the daily output of general circulation models (GCMs) and regional climate models, though analysis of these model outputs across large spatial domains is computationally demanding.

Methods

The objective of this analysis was to map shifts in the distribution of extreme minimum temperatures under future climate projections. The primary challenge was that climate projections are usually provided as monthly means of daily minimum temperatures, following standards for climatological norms. The methods presented here provide an approach to generate projections for minimum temperatures, combining historical records of daily minimum temperatures with standard output from downscaled climate projections (in this case, using the scenarios of the 2008 California Climate Change Impacts Assessment, hereafter CA2008).

Historical climate station data: Daily minimum temperature data was obtained from the U.S. Historical Climate Network for the seven western states (Washington, Oregon, California, Arizona, Nevada, Utah, and Idaho), comprising a total of 245 stations, with data starting from as early as January 1, 1900, and running through December 31, 2010 (locations shown in Figure 2a). Exploratory analyses indicated a fairly high frequency of suspicious data points, usually marked by one-day excursions to unexpectedly low temperatures (e.g., 12°C, -10°C, 14°C on successive days). These were handled by removing all data points with more than a 12°C change from the previous day. The 12°C threshold was chosen based on visual inspection of obvious outliers, while seeking to maintain fluctuations that represent actual variation in day to day temperatures. In addition, several months in values for all days = -17.78°C (= 0°F) were removed, as it appears that 0°F was entered instead of missing data. Subsequent analyses were conducted on this edited data set, and only months with no missing data were used.

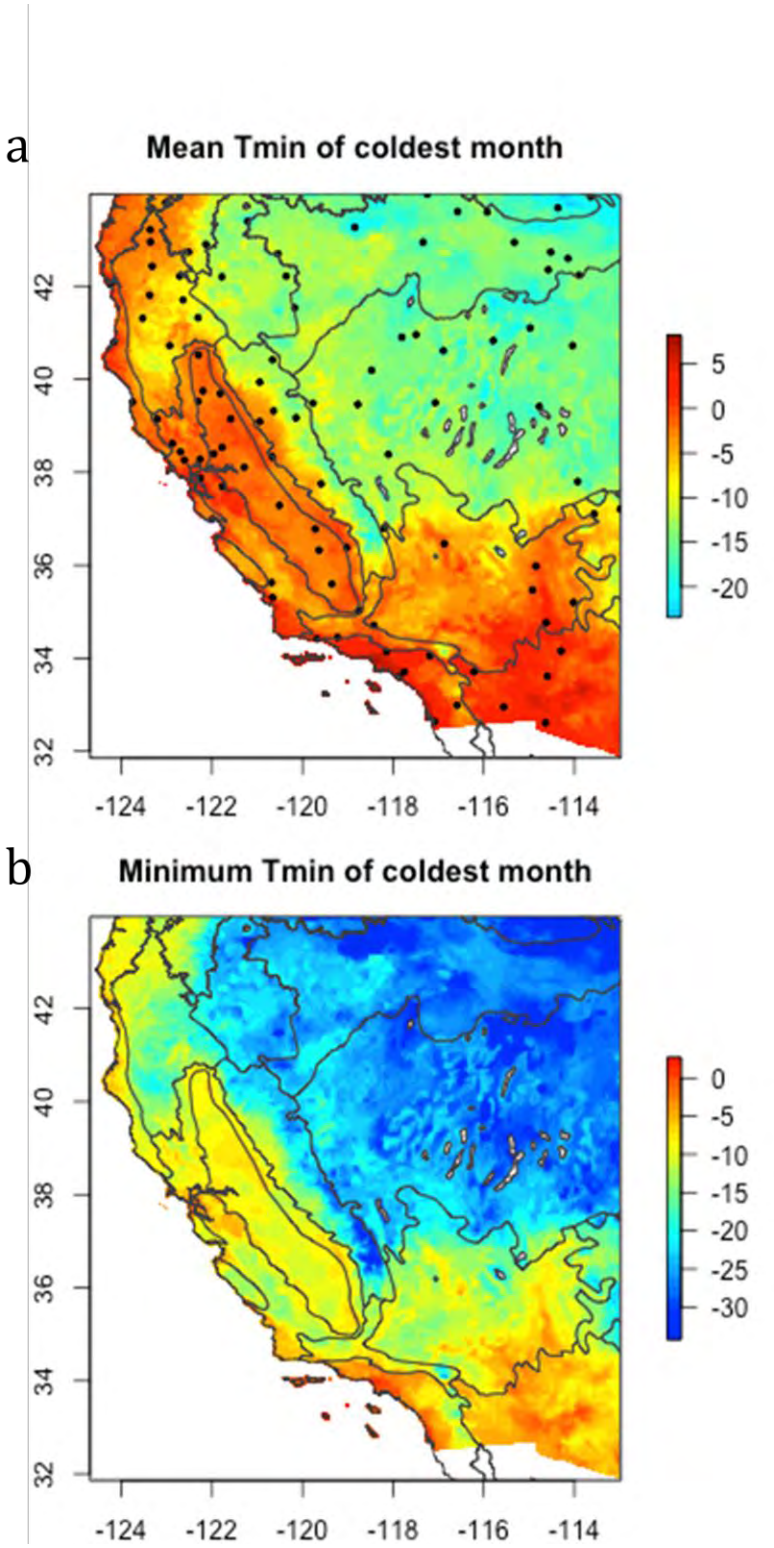

Figure 2. Mean Monthly T_{min} for the Coldest Month in the 1971–2000 Historical Period, from the PRISM Interpolated Climate Surfaces. Solid dots show the position of climate stations in the U.S.

Historical Climate Network. B. Minimum daily T_{min} for the corresponding month in panel A, calculated from Equation 1.1.

For each month, the following statistics were calculated: mean, standard deviation, and minimum for daily T_{min} values, and the percent of days in the month that were less than or equal to four critical values: -10°C, -5°C, 0°C, and +5°C. Minimum and mean monthly T_{min} values are referred to as $T_{min\text{-}min}$ and $T_{min\text{-}mean}$, respectively (Table 1). The resulting data set contained a total of 209,134 monthly climate station records spread fairly equally across the 110-year time span, particularly from 1920 onwards (Figure A1). A plot of $T_{min\text{-}mean}$ vs. $T_{min\text{-}min}$ exhibits slight convex curvature, and an increase in the variance of $T_{min\text{-}min}$ at cold temperatures (Figure 3). Quadratic regression was used to obtain a predictive model for the expected $T_{min\text{-}min}$ as a function of monthly $T_{min\text{-}mean}$ (standard errors of coefficients in parentheses):

$$T_{min\text{-}min} = -6.816\ (0.006) + 1.22\ (9.7E\text{-}4) * T_{min\text{-}mean} - 7.634E\text{-}3\ (6.7E\text{-}5) * T_{min\text{-}mean} \quad (1.1)$$

$$N = 209134,\ R^2 = 0.93$$

In data sets of this magnitude, random partitions into training and test data sets will give indistinguishable results, so this step was not conducted.

Table 1. Abbreviations Used for Minimum Temperature Analysis

Parameter	Definition
T_{min}	Minimum daily temperature
$T_{min\text{-}mean}$	Monthly average of minimum daily temperatures (the conventional method for calculating monthly T_{min} values in climatological data)
$T_{min\text{-}min}$	Minimum T_{min} value over the course of a month (i.e., the coldest minimum daily temperature measured in that month)
$T_{min\text{-}mean\text{-}30}$	Coldest mean monthly T_{min} value observed in a pixel over a 30-year period
$T_{min\text{-}min\text{-}30}$	Coldest monthly minimum T_{min} value observed in a pixel over a 30-year period

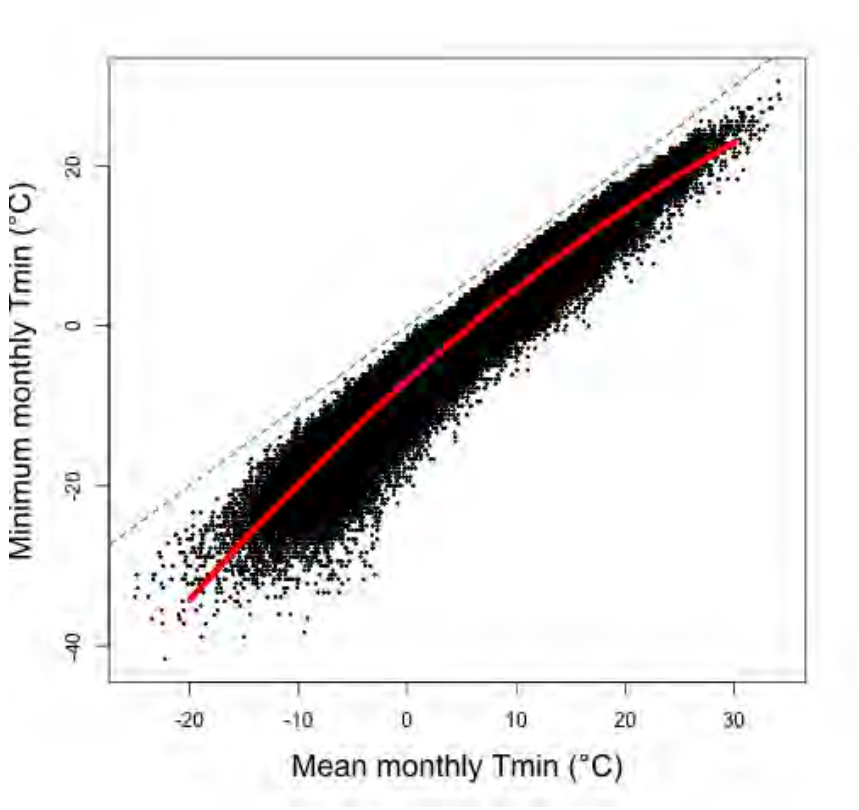

Figure 3. Plot of Minimum vs. Mean Daily T_{min} ($T_{min\text{-}min}$ vs. $T_{min\text{-}mean}$) for All Monthly Data from Western States in the U.S. Historical Climate Network (N = 209,134). The red line shows the best fit quadratic regression (see Equation 1.1).

This function can be used to predict the average coldest temperature expected in a month, as a function of mean monthly minimum temperatures (which are available in climatological summaries and climate projections). At $T_{min\text{-}mean}$ = 0°C, the expected $T_{min\text{-}min}$ is -6.8°C, descending to an extreme $T_{min\text{-}min}$ of -34.3°C when $T_{min\text{-}mean}$ = -20°C. In predictive modeling, this extreme minimum value of -34.3°C was then used for all $T_{min\text{-}mean} \leq$ -20°C, due to the paucity of data points at the lower end of the historical distribution. Because these analyses focused on shifts occurring under global warming scenarios, rather than cooling, the lack of additional data at the cold extremes does not present a problem. In addition, few species exhibit differential responses at these extreme cold temperatures, so changes in $T_{min\text{-}min}$ at these levels are probably not biologically relevant. The calibration data include all months of the year, so they fully span the range of temperatures around 0°C; as a result, projections under future warming do not involve extrapolations.

Several other approaches to analysis of the historical data were considered. Analyses of individual stations, or of data aggregated by month of the year, did not reveal consistent patterns in the resulting regression coefficients. Thus, all data were pooled, and all of the

monthly data points were treated as independent observations. This approach does not take into account spatial or temporal variation in the underlying patterns, which potentially could be incorporated in the interpolations to the regional climate map at the next step. However, it does have the advantage of simplicity, and provides a starting point for other studies that may want to explore minimum temperature patterns if local calibrations from weather stations have not been analyzed.

This study also explored quantile regression to obtain predictive relationships for the minimum temperature that would be expected with a specified frequency. In other words, the 99 percent quantile regression would provide an upper threshold, such that the $T_{min\text{-}min}$ value would be at least that cold in 99 percent of months with a given $T_{min\text{-}mean}$. This approach worked well for the upper quantiles, as the upper edge of the distribution is quite smooth. However, at the lower edge a quadratic quantile regression had strong curvature, leading to inappropriate extrapolations to very negative values at the lower end. A refined statistical approach to fit a predictive function to the lower bounds of this distribution may be warranted.

The percent of days exceeding critical T_{min} thresholds exhibited a sharply non-linear relationship with $T_{min\text{-}mean}$ (Figure 4). As expected, approximately 50 percent of the days in a month experience T_{min} values <= $T_{min\text{-}mean}$. These relationships can be fit fairly well with descending logistic curves (not shown). If desired, these functions could be used to map changes in this statistic across the spatial domain, but these analyses are not pursued further here.

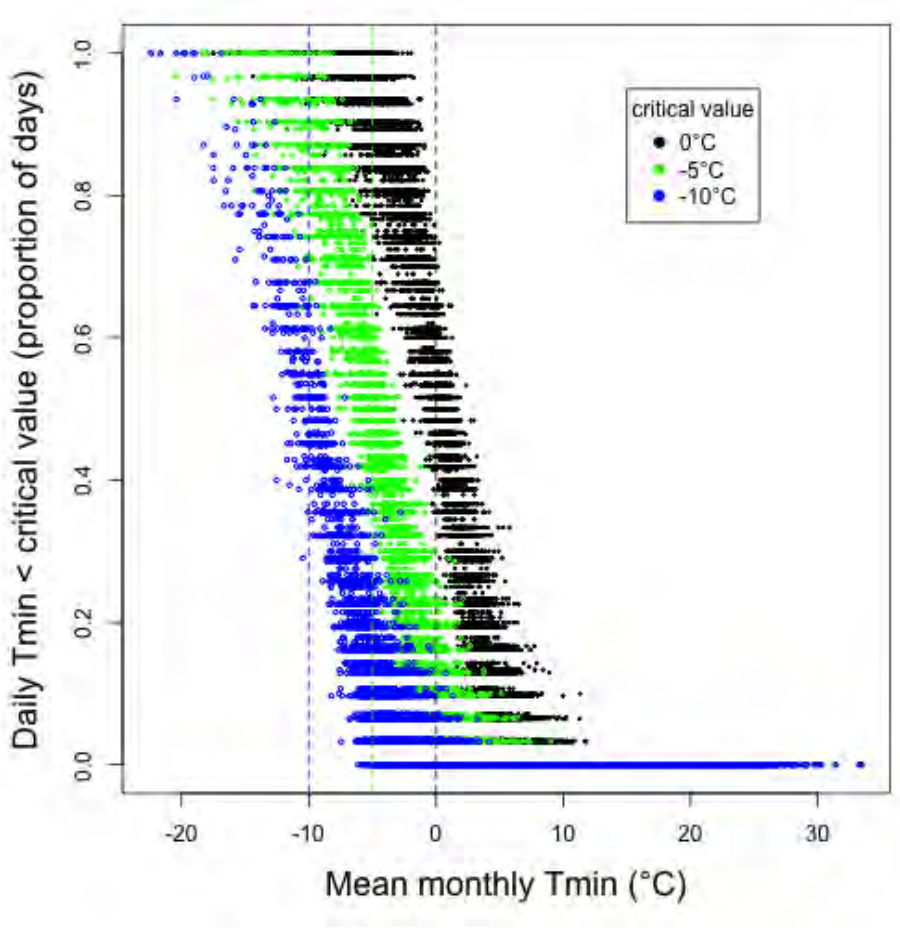

Figure 4. Plot of the Proportion of Days per Month in which $T_{min} < T_{crit}$, vs. Mean Monthly T_{min}. Tcrit = 0°C (black points), -5°C (green points), or -10°C (blue points). For clarity, only N = 20000 points are shown, drawn randomly from the full data set.

Historical norms for mean and minimum T_{min}: The 2.5 arc-minute (~4 km) PRISM[1] data set for the 1971–2000 historical period (Daly et al. 2008) was used to map the current distribution of minimum temperature values for California and adjacent regions, over different time periods (the spatial domain used here follows the area covered by the 2008 California Assessment). Most analyses of seasonal minimum and maximum temperatures focus on January and July or winter versus summer quarters, respectively, often relying on 30-year averages for climatological norms. A slightly different approach was used here to model extreme minimum temperatures over 30-year periods. Using the *raster* library of R (Hijmans and van Etten 2011), a stack was constructed with all 360 monthly $T_{min\text{-}mean}$ PRISM layers, from January 1971 to December 2000. The minimum value was then extracted from the stack for each pixel. The result is a map of the coldest $T_{min\text{-}mean}$ observed over the 30-year period in each pixel, regardless of the month or year

[1] Parameter-elevation Regressions on Independent Slopes Model (PRISM)

in which it occurred ($T_{min\text{-}mean\text{-}30}$, Figure 2a). Equation 1.1 was then used to convert these values to the expected $T_{min\text{-}min}$ that would have been observed in that month, providing a map of the coldest temperature expected over the 30-year historical period ($T_{min\text{-}min\text{-}30}$, Figure 2b). A second stack was then created with $T_{min\text{-}min}$ values for each month, based on Equation 1.1. In each stack, the number of months in which T_{min} values were less than or equal to three critical values (0°C, -5°C, -10°C) was calculated, and then divided by 30 to obtain the average number of months per year in which mean or minimum T_{min} temperatures fall below these levels.

Shifts in the distribution of freezing events under future climate scenarios: The 2008 California Climate Change Impacts Assessment (CA20008) scenarios were used to evaluate changes in the distribution of freezing events under historical versus future climate scenarios. The CA2008 scenarios include the Intergovernmental Panel on Climate Change (IPCC) B1 and A2 emissions scenarios, and are derived from four general circulation models: CCSM3, CNRM, GFDL, and PCM1,[2] downscaled to a 7.5 arc-minute (~12 km) spatial grid (Cayan et al. 2008) .[3] The historical data from these simulations start from 1950 and have been calibrated to match general features of historical climate, but they are not directly tied to interpolated historical records. It is necessary to use the simulations for both historical and future periods to ensure that the differences reflect climate change projections, rather than differences between observations and projections for different periods.

The historical period was defined as 1971–2000, and future periods as early (2010–2039), mid (2040–2069), and late (2070–2099) twenty-first century. Results reported here focus on the late twenty-first century period. For historical and future periods, the same methods were used for analysis, as outlined for the PRISM data above. In each period, the 360 monthly $T_{min\text{-}mean}$ surfaces were stacked, and then converted to a $T_{min\text{-}min}$ stack using Equation 1.1 (under the assumption that the relationship between mean and minimum T_{min} values will be the same under future climates). The coldest $T_{min\text{-}min}$ value over each 30-year period ($T_{min\text{-}min\text{-}30}$), and the average number of months per year in which $T_{min\text{-}min}$ values are lower than critical values (T_{crit}) of 0°C, -5°C or -10°C, were then calculated from this data stack. The resulting maps for the historical period under each CA2008 scenario were compared with the corresponding PRISM maps to determine the similarity in the respective historical baselines.

To assess changes under future climate projections, two sets of maps were then constructed, under each of the four GCMs and the B1 and A2 scenarios, and the three T_{crit} values. The first set showed areas in which $T_{min\text{-}min\text{-}30}$ values were either above T_{crit} or below T_{crit} at least once in both the historical and future period, versus areas where temperatures fell below T_{crit} in the historical

---

[2] Community Climate System Model (CCSM3), Centre National de Recherches Météorologiques (CNRM), Geophysical Fluid Dynamics Laboratory (GFDL), and the National Center for Atmospheric Research (NCAR) Parallel Climate Model (PCM1).

[3] For complete information on CA2008 scenarios, see: http://tenaya.ucsd.edu/wawona-t/cec_adaptation/cec_adaptation_downscaled_data.html.

period but are not projected to fall below T_{crit} in the future period. The latter areas are those that will experience a relaxation of freezing events. The second set of maps was similar, but showed the regions that experienced these three conditions on average one or more times per year, rather than at least once in the 30-year period. As the four GCMs were generally similar, the full results are shown in the appendix, and results of the CCSM3 GCM are illustrated in the main paper.

Results

Historical norms for mean and minimum T_{min}: The distribution of the coldest monthly $T_{min\text{-}mean}$ values for the 1971–2000 period, based on PRISM, is shown in Figure 2a, and the corresponding values for $T_{min\text{-}min}$, based on Equation 1.1, are shown in Figure 2b. The overall pattern in these two maps is virtually identical, as the predictive equation is nearly linear, with a shift towards colder minimum temperatures for $T_{min\text{-}min}$. As expected, the mildest T_{min} values occur along the coast (especially in the San Diego-Los Angeles region and the San Francisco Bay Area) and in the warm Sonoran desert areas. $T_{min\text{-}min}$ values are below zero across almost the entire region, except for portions of the south coast and Imperial Valley, reflecting the fact that the entire area has been subject to at least occasional frost under historical climate conditions. The border between the Mojave and Sonoran deserts roughly follows an isocline of $T_{min\text{-}min}$ ~ -8°C, and between the Mojave desert and Great Basin at $T_{min\text{-}min}$ ~ -20°C. The sharp transitions from the Central Valley to chaparral woodland and Sierra Nevada forests also mirror a steep gradient in minimum temperatures.

The number of months per year in which $T_{min\text{-}mean}$ and $T_{min\text{-}min}$ have fallen below various critical values are shown in Figure 5. As seen in Figure 5b, there are fairly extensive regions of the high mountains and Great Basin in which freezing temperatures are expected in 10 or more months of the year. Freezing events below -5°C, and especially below -10°C, are rare or absent across most of coastal California and the Mojave and Sonoran deserts (Figure 5d, f).

PRISM climate layers were aggregated to match the resolution of the CA2008 scenarios, to allow a pixel-by-pixel comparison across the spatial domain. The 30-year $T_{min\text{-}mean}$ values from the CA2008 scenarios tend to be lower than the corresponding values from the PRISM interpolated layers, especially for the CCSM3 GCM (Figure A2). These discrepancies were greatest in high elevations and interior regions (Figure A3), indicating that the GCMs tended to infer relatively colder temperatures in these areas. As there are few climate stations at high elevations, the PRISM interpolations are known to be less reliable in the mountains, so from this analysis it is not apparent which values are closer to being correct. It does mean that the CA2008 analyses start from a cooler baseline, especially in the mountains, which should be considered when looking at the projected shifts in freezing patterns.

Number of months per year below critical T_{min} (1971-2000)

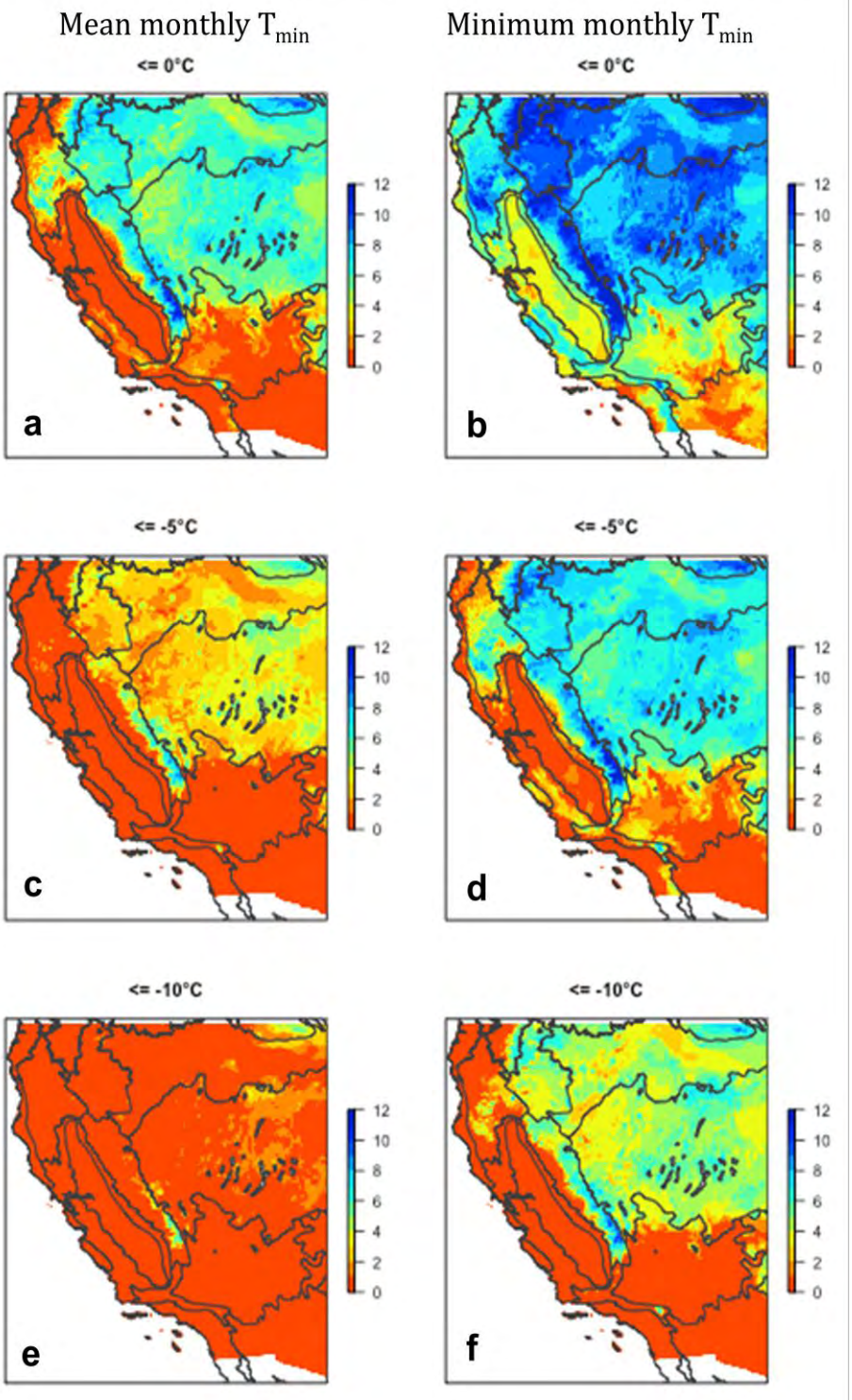

Figure 5. Number of Months per Year (Averaged over 1971–2000) in which Monthly T_{min} Values Fall below Various Critical Levels. a, b: 0°C; c, d: -5°C; e, f: -10°C. a, c, e: Mean monthly T_{min}; b, d, f: Minimum monthly T_{min}.

Changes in the distribution of freezing events under future climates: Figures 6 and 7 illustrate the projected shifts in the distribution of freezing events across California and adjacent areas, comparing 1971–2000 to 2070–2099 for the CCSM3 A2 projections (full results from all GCMs are in Figures A4–9). These maps are all based on the expected $T_{min\text{-}min}$ values, calculated from $T_{min\text{-}mean}$ values in the CA2008 climate layers together with Equation 1.1. The six panels show freezing events below critical values of 0°C, -5°C, or -10°C (32°F, 23°F, or 14°F), occurring either at least once in the 30-year period (Figure 6) or at least once per year (on average, Figure 7). On each map, blue indicates areas that have experienced temperatures below T_{crit} in the historical period, and will continue to in the future; gray are areas that have not experienced temperatures below T_{crit}, and will not experience them in the future; and red shows the transitional zones, which have experienced freezing below T_{crit} in the past, but are not projected to experience these temperatures in the future.

As expected, warming leads to larger areas being relieved from freezing events under the higher emissions A2 scenarios, compared to B1 (right versus left, respectively, in Figures 6, 7, and A4-9). Variation among the four GCMs is relatively minor.

Virtually all of California and surrounding areas have experienced freezing temperatures ($T_{crit} \leq 0$°C) at least once during 1971–2000 (Figure A4) and will continue to at the end of this century. Small areas along the south coast and in the Imperial Valley are projected to be entirely frost free under the A2 emissions scenario. With the exception of these same areas, most of the region has also experienced freezing events at least one month of the year (Figure A5). In the future, especially under the A2 scenarios, increasing areas of the Sonoran desert, the south and central coast, and (under some scenarios) the Central Valley, will be frost free in at least some years.

The south coast and Sonoran desert areas have not experienced freeze events < -5°C in the historical period (Figure A6), and expanding zones around these areas are projected to be entirely free of freeze events below this temperature. Most of southern and coastal California (except at high elevations) and the Central Valley have not experienced freezes ≤ -5°C on an annual basis. This zone expands into the western and northern Mojave desert, up the western slope of the Sierra Nevada, and under most A2 scenarios up into the Coast Range mountains between the Bay Area and Santa Barbara (Figure A7).

The distribution of freeze events < -10°C once in 30 years is similar to <-5°C once per year (Figure A8 versus A7). Under CCSM3 A2, freeze events of this magnitude are modeled for the historical period in the Central Valley, but this is not observed in the PRISM historical layers (Figure 5). At this temperature, a growing area of the northwest coast is projected to no longer experience freeze events in the future. Most of California, except for high mountains, does not experience events < -10°C each year (Figure A9). With warming temperatures, narrow bands around the edges of the Mojave desert, along the western slope of the Sierra, and around the

Klamath-Siskiyous, where such events have occurred historically, will no longer experience them each year.

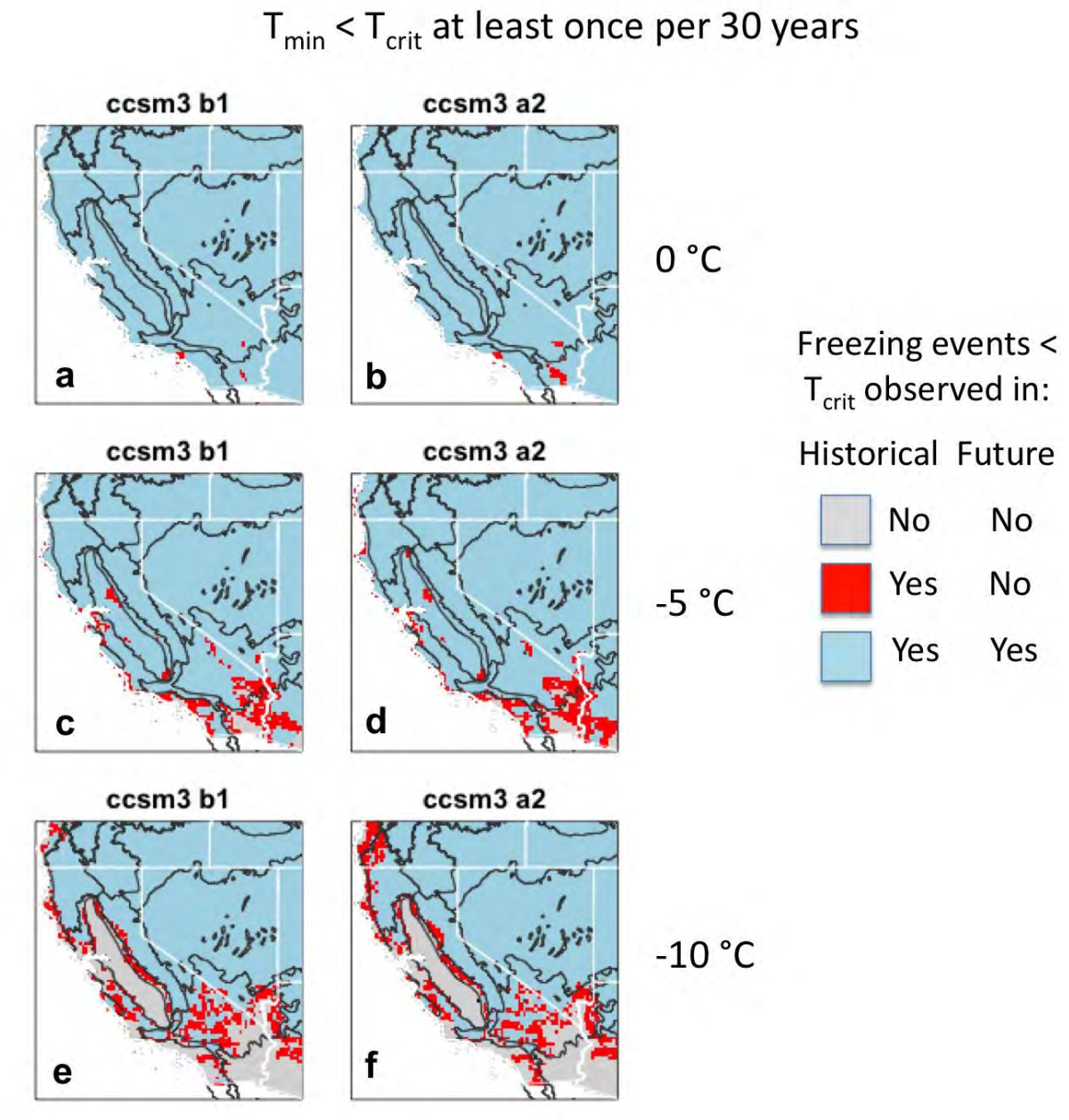

Figure 6: Changes in the Distribution of Freeze Events Occurring at Least Once per 30 Years, from the 1971–2000 Historical Period to the 2071–2100 Future Projections, for the CCSM3 GCM. a, b, d: B1 emissions scenario; c, e, f: A2 emissions scenario. a,b: Freezing events less than critical temperature (T_{crit}) = 0 °C; c,d: T_{crit} < -5 °C; e,f: T_{crit} < -10 °C. Blue areas have experienced a freeze less than the indicated T_{crit} values in the past, and are projected to continue to experience these events in the future. Red areas have experienced these in the past, but are not projected to

experience these in the future. Gray are areas that have not experienced a freeze at this temperature in the past, and will not in the future either.

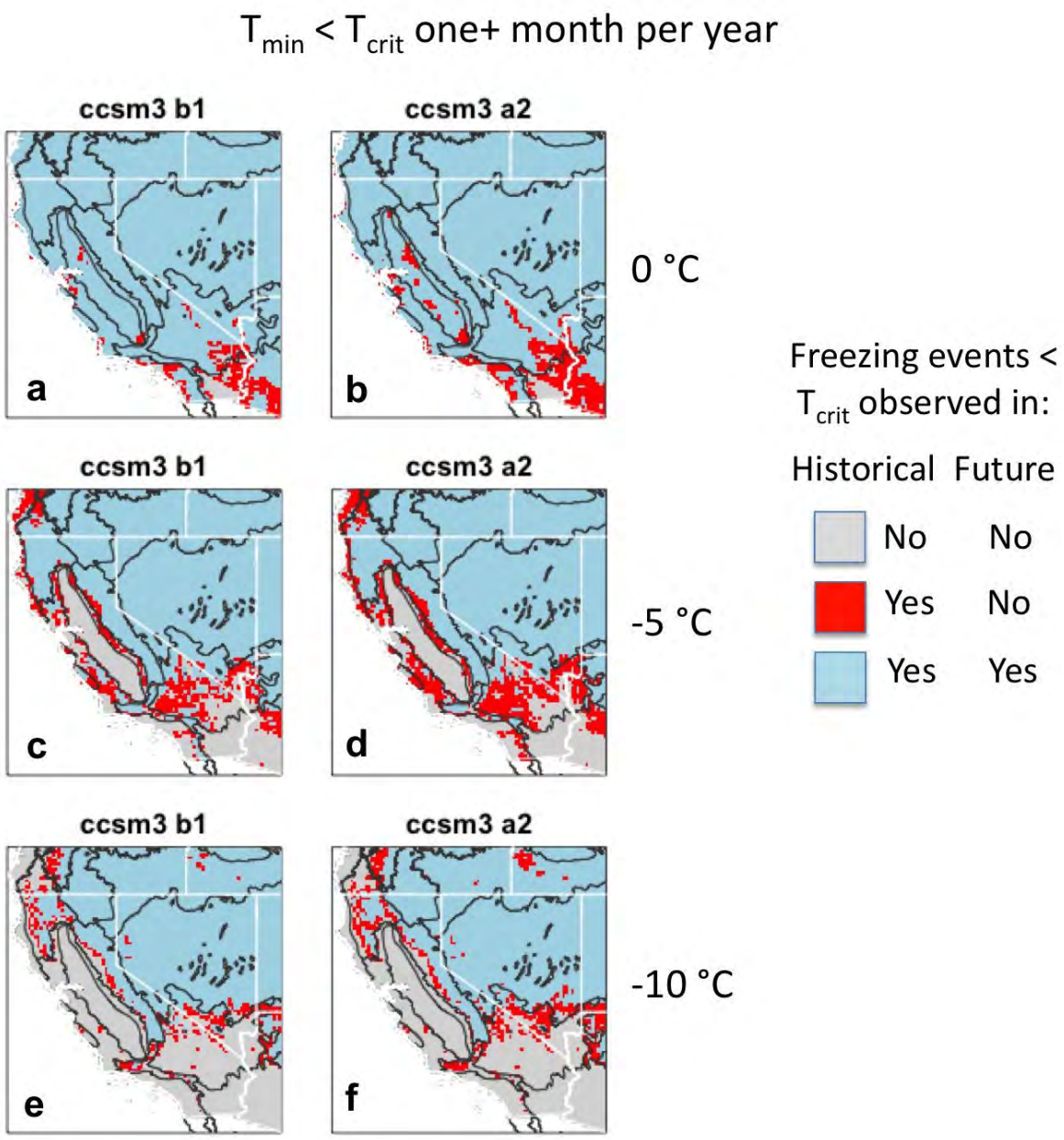

Figure 7. Same as Figure 6, for Freezes Occurring on Average One or More Times per Year

Discussion

Overall, the areas that will experience a relaxation from freeze events of a particular severity and frequency are relatively small (the red areas on the maps). For plants and animals sensitive to

frost (both native and alien taxa), these bands represent key transitional areas in which range expansions and vegetation type transitions could be observed over time. At $T_{crit} < 0°C$, these transitional areas are primarily in the Sonoran desert and along the coast. At colder temperatures, a zone along the western slope of the Sierra Nevada warms above the critical temperatures, along with portions of the Mojave desert, the southern and central coast, the Coast, Transverse, and Klamath-Siskiyou Ranges, and the Central Valley. To the extent that Mediterranean-type vegetation (e.g., chaparral) is limited by occasional freeze events, this may represent opportunities for upslope migration. On the western slope of the Sierra Nevada, vegetation transitions have been observed in the twentieth century, with oak woodland spreading upwards, displacing pine forests (Thorne et al. 2008). Such transitions are expected to continue, though the relative role of changes in winter cold versus summer heat and drought, and succession following land-use changes are difficult to unravel.

Changes in the distribution of freezing events have potentially significant implications for agricultural production as well. In Southern California, the appearance of frost-free areas could allow the introduction of tropical crops. Like native vegetation, crops with particular temperature requirements, or sensitivity, may need to be moved upslope. In contrast to the focus on freezing events here, stone fruits have a well-defined chilling requirement and warming trends may greatly shrink the areas in which they can be produced, especially in the Bay Area and Central Valley (Luedeling et al. 2009).

There are several important points to keep in mind regarding interpretation of these projections. First, for simplicity, this study focused only on the extreme minimum temperatures over the entire year, or over 30-year periods. Of necessity, these values may only be directly relevant for woody plants, and for animals active or at least exposed to winter temperatures. It is well known that cold and freezing sensitivity in plants and animals exhibit striking seasonal acclimation, with greater tolerance developing during cold periods (Kalberer et al. 2006). As a result, unseasonal cold or freezing events, such as a late spring or an early fall freeze, can have much greater negative impacts on plants and animals, even if they are able to tolerate colder temperatures during winter (Gu et al. 2008). Modeling climate change impacts of such unseasonal extreme events is possible in principle, but the analyses would be most useful if calibrated to known physiological sensitivity of a particular species.

A second point to note is that these analyses utilized downscaled climate projections at a 12 km grid cell size. Thus, the patterns reflect only broad mesoclimate trends across geographic and elevational gradients. At finer scales, topographic phenomena such as cold air pooling can generate local freeze events that are substantially decoupled from regional climate (Lundquist et al. 2008). These topographic inversions influence vegetation distributions, in some cases leading to exclusion of cold-sensitive species from low-lying valleys (Davis et al. 2007). In southern California, mortality of cold-sensitive chaparral shrubs has been observed in valleys, even fairly near the ocean, during unusual cold spells (Davis et al. 2007). Inversions have well-known effects in agriculture, as cold-sensitive crops can sometimes only be grown on along the slopes

of low-lying valleys, and not at the bottom. These effects will be important to consider in modeling landscape-scale climate and climate change impacts on biota.

The approach used here, combining the daily records of historical climate stations with the mapping of mean temperatures, is valuable as a first approximation of minimum temperatures experienced over different time scales. However, it is important to note that the estimation of the minimum T_{min} values ($T_{min\text{-}min}$) was based on the expectation of the coldest temperature experienced in a month, as a function of mean monthly T_{min} ($T_{min\text{-}mean}$) (Equation 1.1). As shown in Figure 3, $T_{min\text{-}min}$ has a range of 10°C to 20°C (50°F to 68°F) around the mean, with especially cold $T_{min\text{-}min}$ (relative to the expectation) occurring at low mean monthly T_{min}. As a result, the mapping of areas as entirely frost free (especially over 30-year periods) is only approximate, and rare cold events are still inevitable. This is one reflection of the general problems encountered in projecting the frequency and distribution of extreme events.

In general, discussions of climate change impacts tend to focus on the increase in abiotic stressors impacting natural and human systems, such as heat waves, drought, and extreme precipitation events. The changing distribution of cold temperatures, and especially freezing events, lies on the opposite end of the spectrum; cold is a factor that may have restricted some species from occupying regions historically, and this restriction will now be relaxed. This raises the question of what ecological processes may contribute to biotic responses to this relaxation. For example, if there are tradeoffs between cold tolerance and growth rate, or competitive ability, then less cold-tolerant plants may be able to invade new sites and gradually outcompete existing vegetation. However, in the absence of factors that directly and negatively affect existing plants, such direct competitive displacement could be impeded by priority effects and the absence of opportunities for establishment of new taxa. Alternatively, replacement of cold-tolerant by less cold-tolerant taxa may primarily occur following disturbances, such as wildfire or drought-induced mortality of existing vegetation (Allen et al. 2010). Of equal importance, relaxation of freezing limits will allow for expansion of cold-sensitive crops (e.g., vineyards, avocados) into undeveloped areas, leading to new patterns in land-use change. Observational studies of vegetation dynamics in coming decades will be critical to better understand the mechanisms underlying climate change impacts on natural vegetation.

Section 2: Mapping Disappearing and Novel Climates under Future Climate Scenarios

The climate of a particular place on the globe reflects long-term average values for individual climate variables (minimum and maximum temperatures, precipitation, length of dry season, etc.) as well as the frequency and intensity of extreme events. While plant and animal distributions, physiology, and demography are clearly influenced by climate, we often do not know which aspects of climate affect which species. This uncertainty has led to development of methods to map and quantify the overall severity of climate change as a guide to the magnitude of potential impacts (Williams et al. 2007; Loarie et al. 2009; Ackerly et al. 2010; Klausmeyer et al. 2011; Davison et al. 2012).

One principle guiding these analyses is the idea that the impacts of a particular aspect of climate change should be scaled by the historical variability in the parameter of interest, on the assumption that biological systems will exhibit a certain amount of resilience in response to "normal" levels of historical variability. At a local scale, if future climate exceeds the range of historical variability in one or more parameters, we can say that organisms will experience a novel climate, though the exact threshold used to specify "novelty" will depend on the time frame and measures used to quantify historical variability. At a regional (or global) scale, future climates that exceed the historical range observed anywhere in the spatial domain can be considered novel at that scale; i.e., climate conditions projected for the future do not resemble the climates currently observed anywhere in the region. Similarly, by quantifying the extent of particular climate types, we can also classify certain climates as shrinking, expanding, and disappearing, when comparing a future period (under a particular climate change scenario) with the historical baseline.

Due to the multivariate nature of climatic variation, only a small number of the possible combinations of different factors will actually exist. For example, in California there are very hot areas (in the deserts) and very wet areas (in the northwest), but the combination of hot and wet (which would correspond to a tropical rain forest environment) does not exist. Jackson and Overpeck (2000) coined the term "realized environment" to refer to the combinations of climate conditions that exist at a given time. Changes in the availability or distribution of realized environments are likely to have significant biotic impacts at a regional scale, as organisms may no longer find suitable conditions, or may not be able to disperse rapidly enough to track rapidly changing conditions. Novel climates pose an additional challenge, because we have no analogs (at least within the domain of interest) to use as a basis for projecting the kinds of species or communities that would be expected under the novel conditions.

Williams et al. (2007) pioneered the analysis of novel climates. They calculated the multivariate standardized Euclidean distance (SED) between the climates of each pixel, globally, relative to all other pixels, using four climate variables, where the distance for each variable was scaled by its interannual standard deviation from 1980–1999. Novel climates were classified as those points where the future climate was more than 3.22 SED units from any point on the globe at present, averaged over several GCMs for the late twenty-first century. Conversely, disappearing climates were those in which the current climates exceeded this threshold, relative to any future value. They also mapped locally novel and disappearing climates, by comparing each pixel to those within a radius of 500 km. At a global scale, under the A2 scenario, novel climates were primarily located in tropical lowlands, and disappearing climates in tropical mountains. One pixel that appears to be near the San Francisco Bay Area is classified as novel. When the analysis is restricted to the 500 km radius, several pixels along the California coast appear as novel climates.

Wiens et al. (2011) recently published an analysis of novel and disappearing climates, focused on California. They constructed a principal components analysis (PCA) from eight climate variables and then used the first two PCA axes for their analysis. They calculated a bivariate

density surface in this two-dimensional space and drew polygons around the areas containing 99.9 percent of the pixels. Novel climates were defined as those conditions, under future climate scenarios, that fell outside of these polygons, while disappearing climates were those that were no longer represented in the future. The future climates projections were obtained from a regional climate model for the mid-century period from 2038–2069 under the A2 scenario. They found small areas of disappearing climates on the North Coast and in areas surrounding Mono Lake and Death Valley. Fairly extensive areas of novel climate appeared in the Sonoran and Colorado Deserts, and in portions of Death Valley and the Mojave Desert. Interestingly, novel climates also appeared in the Central Coast mountains, where the regional climate model projects cooler and wetter future conditions.

Ackerly et al. (2010) developed a different approach that has elements of the two above. They selected two climate variables for simplicity—mean annual temperature and total annual precipitation—and constructed a two-dimensional histogram of existing climate variation, where the width of the histogram bins on each axis were set to three times the average standard deviation for each variable during the 1971–2000 historical period. Future climates representing new combinations of temperature and precipitation (i.e., histogram bins that were unoccupied in the past) were classified as novel, and those that no longer occur were classified as disappearing. This approach also makes it possible to quantify the change in the area occupied by persisting climate types, and to determine if they are shrinking or expanding in extent. The analysis was run with two future climate projections, the warmer and drier GFDL_CM2 and the warmer and wetter CCCMA_CGCM3, for the 2070–2099 period under the A1b scenario. The results showed very small areas of disappearing climates in the high peaks of the Sierra Nevada and White Mountains, and novel climates along the South Coast and the San Joaquin Valley. In addition, hot conditions in the southern Central Valley and low-lying coastal areas expand to occupy much more extensive areas in the future.

The objective of the present study was to map the distribution of disappearing, shrinking, expanding, and novel climates for the State of California, following the methods of Ackerly et al. (2010), under future climate scenarios provided by the 2008 California Climate Change Impacts Assessment (see Cayan et al. 2008). The results were then used to evaluate the climatic overlap (comparing historical and future conditions) of parks and other protected areas across the state (Section 3). As the review of previous studies demonstrates, the results of these analyses are quite sensitive to the methods, the choice of climate variables, and the spatial domain. The rationale for the choices made in this study are outlined here.

1. *Spatial Domain*: The idea of a disappearing or novel climate can only be framed in the context of a particular spatial domain. A climate that disappears from California (e.g., high mountains) may be found elsewhere in the western United States, or the rest of the world, under a future scenario. However, for conservation purposes, if a particular climate disappears within a domain of interest, then any species or ecosystems that are tightly linked to that climate may also disappear. Conversely, a novel climate may be novel in California, but currently exist elsewhere (e.g., the spread of hot deserts more

similar to Arizona or northern Mexico). However, if species that occupy such environments are dispersal limited, then these novel environments in California may be unreachable. In these circumstances, we do not have a strong basis to project what species or ecosystems will occupy such environments in the future when they arise within California. This paper presents results using the 2008 California Climate Change Impacts Assessment 12 km climate projections (CA2008), restricted to the California state domain. Results for the CA2008 California-Nevada domain are presented in appendix figures. The state level analysis is appropriate for planning purposes, as the level of decision-making for state agencies and conservation planners (Wiens et al. 2011). From a biological perspective, a continuous spatial domain with a moving window can be used to assess novel climates, relative to surrounding areas from which species could disperse (for example, the 500 km radius moving window used by Williams et al. 2007). Such methods are computationally quite intensive, and also require a large spatial buffer for calculations at the edges of the domain.

2. *Variable Selection*: The relevance of this analysis to biological impacts will depend on the choice of climate variables and their relevance to plants, animals, and ecosystems. For this analysis, I chose three variables: minimum temperature of the coldest month, maximum temperature of the hottest month, and total precipitation. The rationale is that biological processes, and the range limits of species and ecosystems, will be more strongly affected by temperature extremes than annual averages. Due to the strong marine influence on California's climate, coastal areas have mild winters and cool summers, while interior regions have colder winters and hotter summers. This decoupling of minimum and maximum temperatures means that mean annual temperature is not directly correlated with these seasonal extremes, and is a poor descriptor of temperature gradients. Total precipitation is used as a surrogate for water availability because most of the state has a Mediterranean climate, so the seasonal distribution is broadly similar. This is not true for analyses over the broader western U.S. domain, as there is relatively more summer rainfall in interior and desert regions. In the future, I plan to run these algorithms on the 270 m downscaled data from Flint and Flint (2012), using climatic water deficit rather than precipitation. Analyses parameterized for specific taxa or ecosystems may require consideration of additional or a different set of variables, depending on the climatic sensitivity of the study system.
3. *Classifying Climate Types*: The third problem is how to scale variation in different climate variables and create discrete "climate types," or isoclimates, thus allowing identification of which types are disappearing, shrinking, expanding, and novel. Williams et al. (2007) examined on a pixel-by-pixel basis the standard deviation of annual values for each climate variable over the historical baseline period, and scaled the changes in each variable relative to these deviations. This method is used here to calculate and map the magnitude of projected change for each pixel. As discussed above, I simplified the approach for analysis of novel climates, following Ackerly et al. (2010), and used the historical standard deviations to define the widths of bins for each climate variable, and then calculated multidimensional histograms of the frequency (= area occupied) of

different climates. This allows a more rapid calculation of which climate types are shrinking, expanding, disappearing, and novel, relative to the entire spatial domain. This approach is implemented here, using the CA2008 projections, with a larger bin width of four standard deviations, so that isoclimates are classified more broadly and the assessment of novel and disappearing climates is more conservative.

Methods

Spatially interpolated maps for current and future climates at a 7.5 arc minute scale were obtained from the 2008 California climate change impacts assessment report (Cayan et al. 2008). These layers span a spatial domain from the Pacific Coast to 113°W longitude and the Mexican border to 44°N latitude, including all of California and Nevada and small areas of surrounding states. Mean minimum monthly temperature (T_{min}), mean maximum monthly temperature (T_{max}), and total monthly precipitation (P_{tot}) were obtained for each month for the years 1971 to 2099, for four general circulation models—CNRM, GFDL, PCM1, and CCSM3—and two IPCC emissions scenarios (B1 and A2). The B1 scenario involves significant reductions in fossil fuel burning and stabilization of atmospheric CO_2 levels at about 500 parts per million (ppm), with increases of 1.1°C –2.9°C (2.0°F–5.2°F) in global surface temperature by the end of the century. The A2 scenario represents continued growth in greenhouse gas emissions, with atmosphere CO_2 levels over 800 ppm, and global surface temperatures rising 2°C–5.4°C (3.6°C–9.7°C). Current emissions trajectories are at or above those used in the higher A2 scenario (Raupach et al. 2007). Note that the historical and future layers all represent downscaled output from GCM runs, and are not spatially interpolated surfaces based on climate station data. It is important to use model output for both periods so that changes from past to future reflect climate change projections, and not differences between interpolated and modeled data.

For each year, the twelve monthly maps were "stacked" to calculate annual statistics: the minimum value for T_{min}, maximum value for T_{max}, and sum for P_{tot}. These calculations were conducted "pixel-wise" so, for example, the minimum values across the map did not necessarily have to occur in the same month in each pixel or in each year (in contrast with analyses that utilize January minimum and July maximum temperatures). Total annual precipitation values were log10-transformed for subsequent analyses (P_{Ltot}), due to the skewed distribution of precipitation, both spatially and for interannual variation. Thirty-year climatological norms were then calculated as the average of the annual values for the three statistics, for four periods: 1971–2000, 2010–2039, 2040–2069, and 2070–2099. Analyses presented here focus on the first and last intervals as the "historical" and "future" periods.

The magnitude of climate change, relative to historical variability, was calculated as the standardized Euclidean distance between the future and historical climate values, scaled by the historical variance for each climate variable (Williams et al. 2007):

$$SED = \sqrt{\sum_{k=1}^{3} \frac{\left(X_f - X_h\right)^2}{s_h^2}}$$

where k represents the climate variable (T_{min}, T_{max}, or P_{Ltot}), X_f and X_h are the future and historical mean values in a given pixel, and s_h^2 is the interannual variance during the historical baseline period (Figure 8).

Isoclimates were defined by assigning each pixel to a bin in a three-way table for T_{min}, T_{max}, and P_{Ltot}. The width of the bins was based on the magnitude of historical variability for each parameter. Historical variability was calculated as the standard deviation of the annual values for the 1971–2000 period, averaged over the spatial domain. For each variable, the bin width was then set to four times the temporal standard deviation (providing a more conservative assignment of novel isoclimates, compared to Ackerly et al. 2010), and the necessary number of bins was assigned to span the range of climate conditions in the historical and future periods. The number of bins varied among the eight scenarios, due to differences in modeled variability, the magnitude of climate change, and whether the analysis was conducted over the entire California-Nevada domain, or restricted to the State of California. For each scenario and domain, historical and future climates were assigned to their respective bins in this three-way table, and each climate type was then assigned to one of six fates: (1) disappearing, (2) shrinking by more than 10-fold in area, 3) shrinking by 1- to 10-fold, (4) expanding by 1- to 10-fold, (5) expanding by more than 10-fold in area, or (6) novel.

For example, for the CCSM3-A2 scenario for California, there were six bins for T_{min}, nine bins for T_{max}, and four bins for P_{Ltot}, for a total of 216 potential isoclimates (Table 2). Only 60 of these potential isoclimates were observed in the 1971–2000 period, and 66 in the 2070–2099 period. Of the 60 isoclimates in the historical period, 16 were not observed in the future, and were classified as disappearing climates. Six isoclimates shrank by more than 10-fold in area and 22 by 1- to 10-fold; 12 types expanded by 1- to 10-fold, and 4 expanded by more than 10-fold. Finally, 22 of the bins were empty in the historical period, but observed in the future, and were classified as novel climates. Most of the novel climates involve increases in minimum temperatures at low precipitation levels, reflecting winter warming in desert regions (Table 2). Each pixel on the historical climate map can then be assigned to one of the first five types (by definition, novel climates do not exist in the present), and each pixel on the future climate map assigned to one of the last five (disappearing types do not exist in the future).

Table 2. Three-dimensional Histogram for Areas Occupied under Historical (left) and Future (right) Climates for the California State Domain (future in this example if CCSM3, A2, 2070–2099). The four subtables represent different precipitation levels (left column) and within each subtable, rows represent bins of maximum temperature and columns are bins of minimum temperature (row and column labels show lower cutoffs for each bin). Values are the number of pixels occupied by each combination of climate values, where pixel size is 7.5 arc min, approximately 12 km on a side. Cells colors show fate of each climate, comparing historical and future values (and correspond to colors in Figures 10 and 11): gray = disappearing climate; dark blue = >10-fold reduction in area; light blue = 10- to 1-fold reduction; yellow = 1- to 10-fold expansion; orange = >10-fold expansion; red = novel climate.

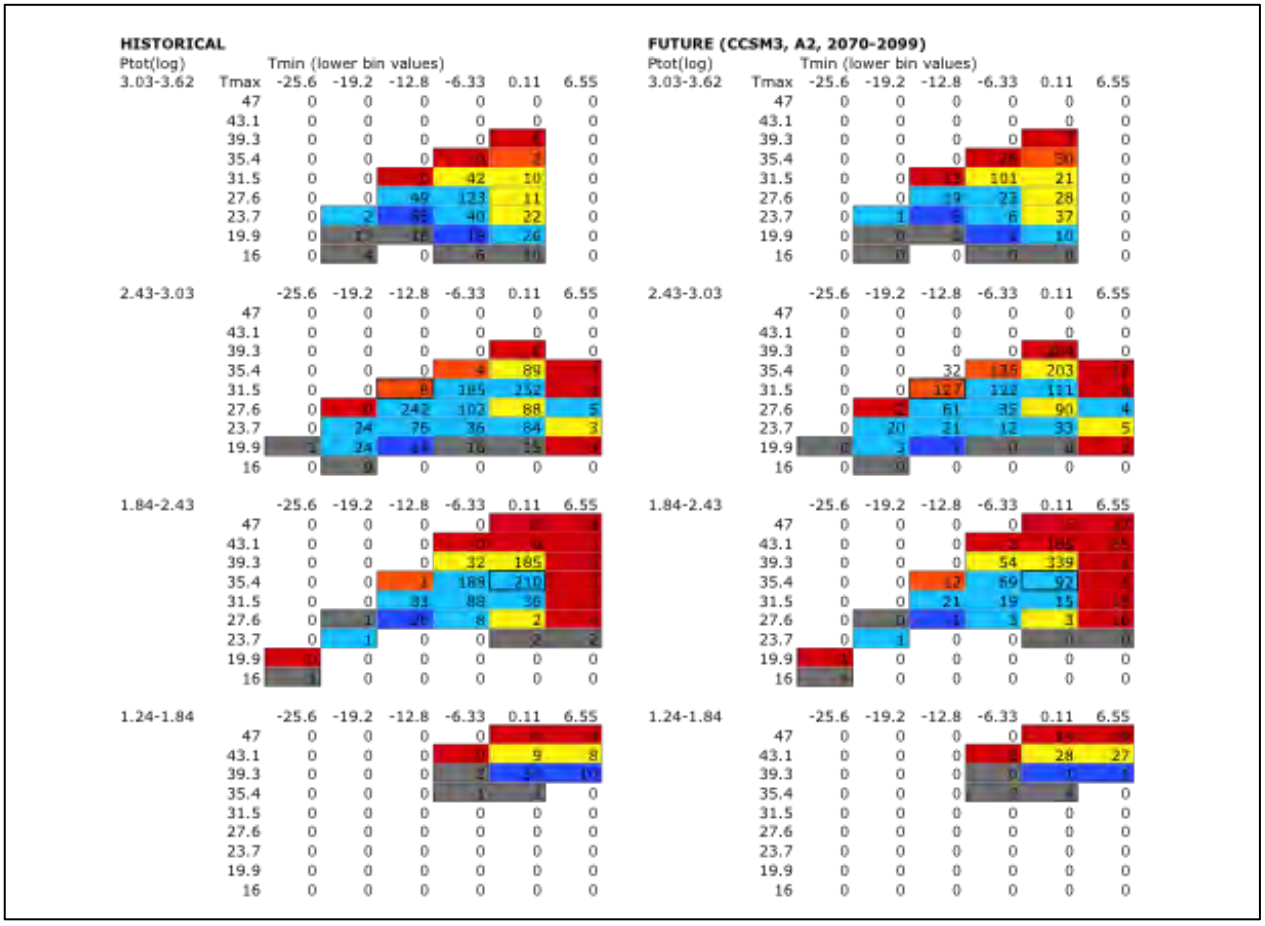

HISTORICAL

Ptot(log)	Tmax	Tmin (lower bin values)					
		-25.6	-19.2	-12.8	-6.33	0.11	6.55
3.03-3.62	47	0	0	0	0	0	0
	43.1	0	0	0	0	0	0
	39.3	0	0	0	0	[illegible]	0
	35.4	0	0	0	[illegible]	[illegible]	0
	31.5	0	0	[illegible]	42	10	0
	27.6	0	0	49	123	11	0
	23.7	0	2	[illegible]	40	22	0
	19.9	0	[illegible]	[illegible]	[illegible]	26	0
	16	0	[illegible]	0	[illegible]	[illegible]	0
2.43-3.03		-25.6	-19.2	-12.8	-6.33	0.11	6.55
	47	0	0	0	0	0	0
	43.1	0	0	0	0	0	0
	39.3	0	0	0	0	[illegible]	0
	35.4	0	0	0	[illegible]	89	[illegible]
	31.5	0	0	[illegible]	185	252	[illegible]
	27.6	0	[illegible]	242	102	88	5
	23.7	0	24	76	36	84	3
	19.9	[illegible]	24	[illegible]	[illegible]	[illegible]	[illegible]
	16	0	[illegible]	0	0	0	0
1.84-2.43		-25.6	-19.2	-12.8	-6.33	0.11	6.55
	47	0	0	0	0	[illegible]	[illegible]
	43.1	0	0	0	[illegible]	[illegible]	[illegible]
	39.3	0	0	0	32	185	[illegible]
	35.4	0	0	[illegible]	188	210	[illegible]
	31.5	0	0	84	88	36	[illegible]
	27.6	0	[illegible]	26	8	2	[illegible]
	23.7	0	[illegible]	0	0	[illegible]	[illegible]
	19.9	[illegible]	0	0	0	0	0
	16	[illegible]	0	0	0	0	0
1.24-1.84		-25.6	-19.2	-12.8	-6.33	0.11	6.55
	47	0	0	0	0	[illegible]	[illegible]
	43.1	0	0	0	[illegible]	9	8
	39.3	0	0	0	[illegible]	[illegible]	[illegible]
	35.4	0	0	0	[illegible]	[illegible]	0
	31.5	0	0	0	0	0	0
	27.6	0	0	0	0	0	0
	23.7	0	0	0	0	0	0
	19.9	0	0	0	0	0	0
	16	0	0	0	0	0	0

FUTURE (CCSM3, A2, 2070-2099)

Ptot(log)	Tmax	Tmin (lower bin values)					
		-25.6	-19.2	-12.8	-6.33	0.11	6.55
3.03-3.62	47	0	0	0	0	0	0
	43.1	0	0	0	0	0	0
	39.3	0	0	0	0	[illegible]	0
	35.4	0	0	0	[illegible]	[illegible]	0
	31.5	0	0	[illegible]	101	21	0
	27.6	0	0	[illegible]	[illegible]	28	0
	23.7	0	[illegible]	[illegible]	[illegible]	37	0
	19.9	0	[illegible]	[illegible]	[illegible]	10	0
	16	0	[illegible]	0	[illegible]	[illegible]	0
2.43-3.03		-25.6	-19.2	-12.8	-6.33	0.11	6.55
	47	0	0	0	0	0	0
	43.1	0	0	0	0	0	0
	39.3	0	0	0	0	[illegible]	0
	35.4	0	0	32	[illegible]	203	[illegible]
	31.5	0	0	[illegible]	[illegible]	[illegible]	[illegible]
	27.6	0	[illegible]	61	35	90	4
	23.7	0	20	21	12	33	5
	19.9	[illegible]	[illegible]	[illegible]	[illegible]	[illegible]	[illegible]
	16	0	[illegible]	0	0	0	0
1.84-2.43		-25.6	-19.2	-12.8	-6.33	0.11	6.55
	47	0	0	0	0	[illegible]	[illegible]
	43.1	0	0	0	[illegible]	[illegible]	[illegible]
	39.3	0	0	0	54	[illegible]	[illegible]
	35.4	0	0	[illegible]	[illegible]	[illegible]	[illegible]
	31.5	0	0	21	[illegible]	[illegible]	[illegible]
	27.6	0	[illegible]	[illegible]	[illegible]	[illegible]	[illegible]
	23.7	0	[illegible]	0	0	[illegible]	[illegible]
	19.9	[illegible]	0	0	0	0	0
	16	[illegible]	0	0	0	0	0
1.24-1.84		-25.6	-19.2	-12.8	-6.33	0.11	6.55
	47	0	0	0	0	[illegible]	[illegible]
	43.1	0	0	0	[illegible]	28	27
	39.3	0	0	0	[illegible]	[illegible]	[illegible]
	35.4	0	0	0	[illegible]	[illegible]	0
	31.5	0	0	0	0	0	0
	27.6	0	0	0	0	0	0
	23.7	0	0	0	0	0	0
	19.9	0	0	0	0	0	0
	16	0	0	0	0	0	0

The fate of individual climate types can be illustrated by mapping their distribution in the historical and the future period, showing the change in area occupied and location (e.g., Figure 9). These maps are similar to the method of climate analogues, which identified places whose climate is most similar to the future climate of a particular location (Veloz et al. 2011). These analogs provide a particularly intuitive way for non-specialists to grasp the implications of future climate projections.

When all climate types are mapped together, the result is a pair of maps displaying the fate of current climates, and the status of projected future climates (e.g., Figures 10 and 11). The light

blue areas on the left represent areas whose climates are projected to shrink in extent, and to occupy the corresponding light blue areas in the future shown on the right (and similarly for dark blue, yellow, and orange). Black in the present represents areas with disappearing climates, and red in the future is the distribution of novel climates. The relative area assigned to each category (in the historical and future periods) can be determined by summing the number of pixels in the corresponding climate types (the current analysis was conducted on geographic projections, so pixel areas are not exactly identical from south to north). What is not shown by these composite maps is exactly what the climate conditions are in each category. The light blue area may include very different climates in different parts of the domain, and it is not possible in this graphic to display the shifts from historical to future periods for all climate types.

Results

The magnitude of climate change across the California-Nevada domain, scaled by historical variability for the three variables considered here, ranged from 0.81 to 5.3 units under the lower emissions B1 scenarios, and from 1.8 to 10.6 units for the A2 scenarios (Figure 8). The units here represent standardized Euclidean distances, over three variables, so a value of 5 represents an approximate change in the mean for each variable of almost three standard deviations, which would effectively shift future conditions outside the range of historical variability. Changes were more marked under the GFDL and CCSM3 GCMs, compared to CNRM and PCM1; further inquiry is needed to determine the relative contribution of the magnitude of change per se versus differences in levels of interannual variability that are used to scale changes in the different variables. Under the A2 scenarios, change is generally greater in interior regions, particularly the Great Basin, but the patterns are fairly patchy. Relatively high levels of change can be seen along the northwest coast and in southern California under some scenarios and models.

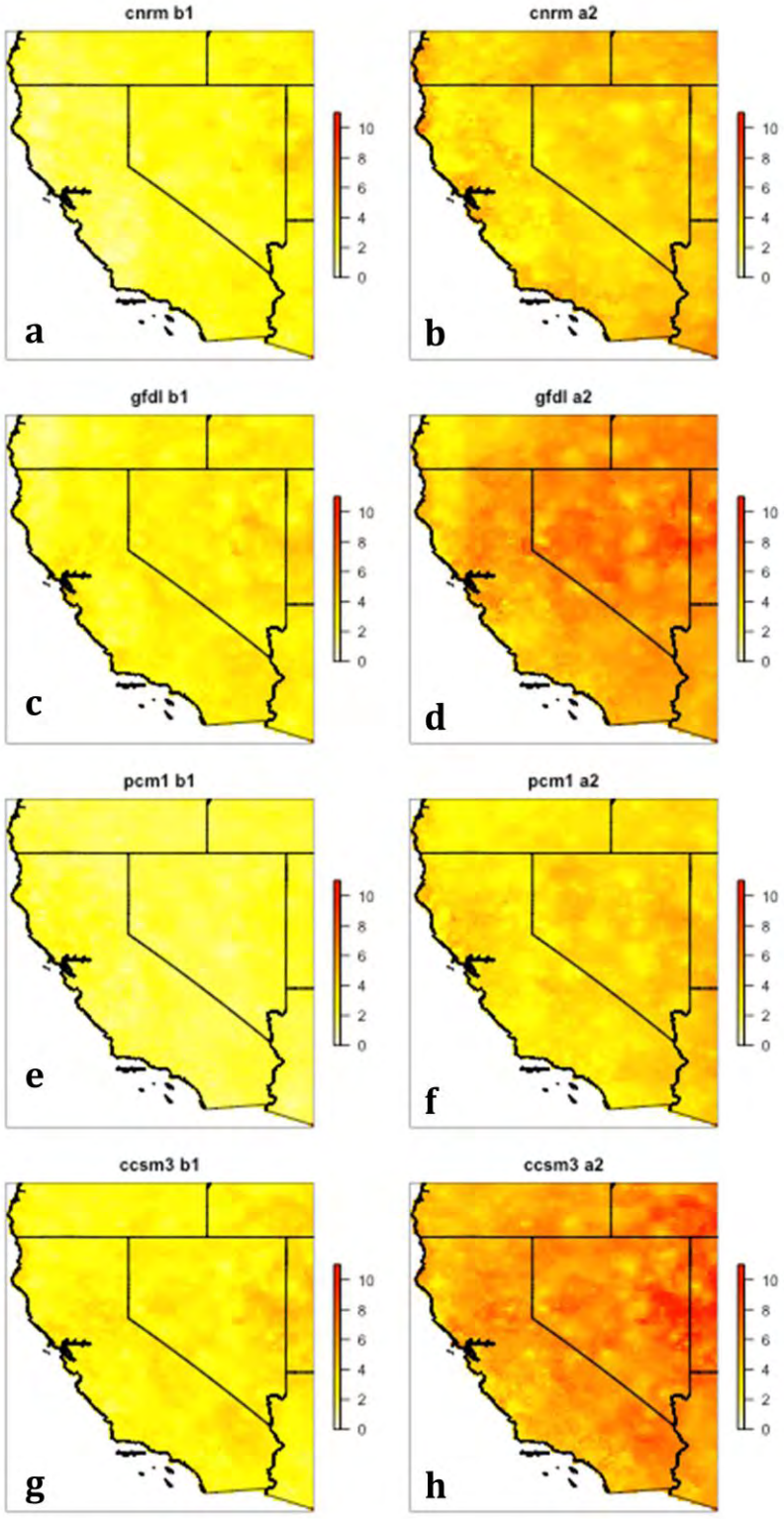

Figure 8. Magnitude of Climate Change for California and Nevada, Measured as the Standardized Euclidean Distance between Historical (1971–2000) and Future (2070–2099) Conditions, Scaled by

Historical Variability. Values > 5 (orange to red) generally represent future conditions beyond the range of historical variability (see text).

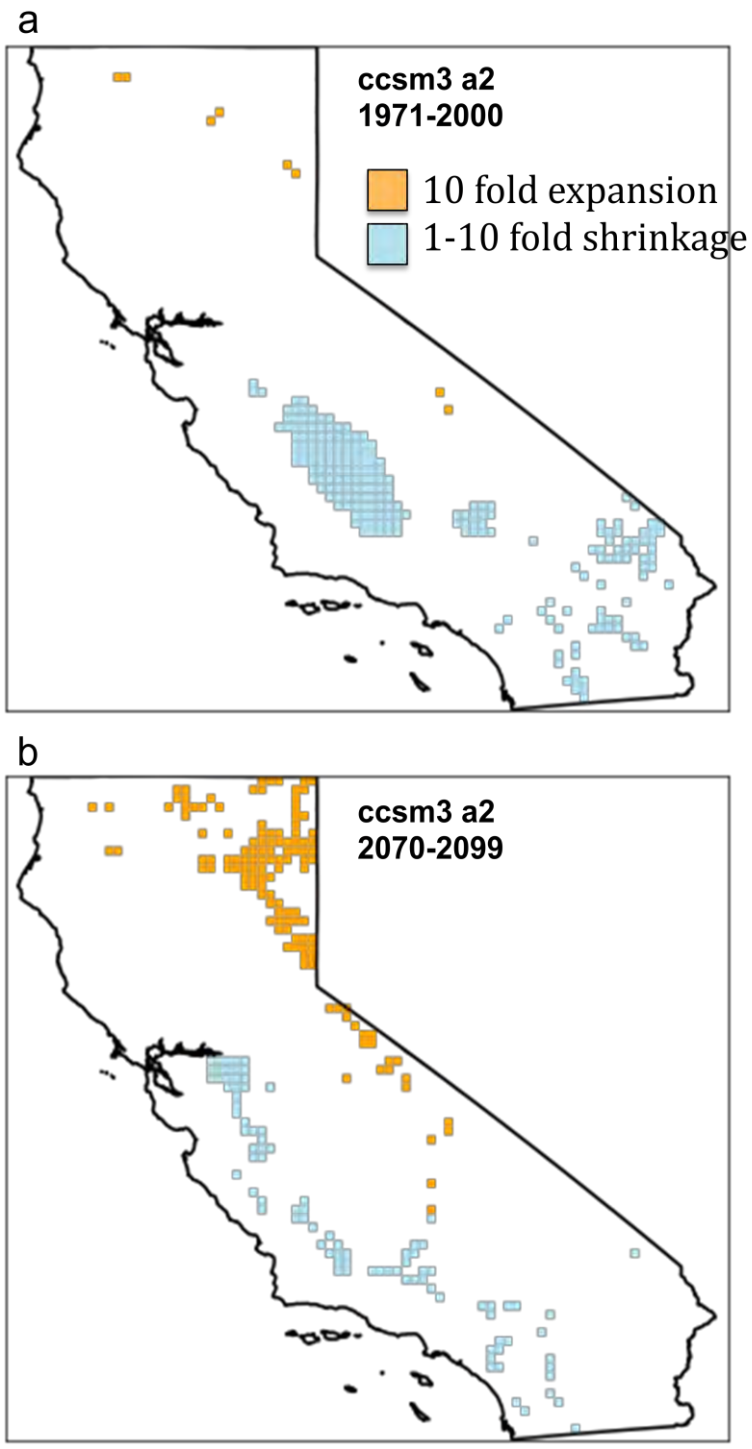

Figure 9. Example of an Expanding and a Shrinking Climate Type, from the CCSM3 A2 Scenario. The two conditions selected for illustration are outlined in black boxes in Table 1. a: Historical

period, 1971–2000. b: Future period, 2070–2099. Orange: precipitation (mm, log) 2.43–3.03, Tmin (°C) -12.8 to -6.3 °C, Tmax (°C) 31.5–35.4, which expands from 8 pixels in the historical period to 127 pixels in the future. Blue: precipitation 1.84–2.43, Tmin 0.11–6.55, Tmax 35.4–39.3, which shrinks from 210 pixels to 92 pixels.

Under B1 emissions scenarios, most isoclimates in California exhibit moderate shrinkage or expansion (Figure 10; see Figure A10 for the larger California-Nevada domain). The distribution of these categories varies among GCMs, especially for the larger spatial domain. When restricted to California, the current climates of most coastal and montane regions are shrinking in extent, while climates of the deserts and Central Valley expand to occupy larger areas. Novel climates appear in the Sonoran desert regions.

Under A2 emissions scenarios changes are more severe and pervasive (Figures 11 and A11). Under two of the four GCMs, significant areas of the Central Valley experience novel climates, unlike any experienced in California during the historical period. Coastal and montane climates shrink, and current climates of the high Sierra Nevada, and of some areas along the coast, disappear entirely. For the broader California-Nevada domain (Figures A11), current isoclimates of the Great Basin shrink dramatically and are replaced by expanding climates from hotter desert regions (see small areas of orange in left panels which expand to extensive orange areas on right, Figure A11). Portions of the Sonoran desert, the Sacramento Valley and the Great Basin experience novel climates.

The nature of novel climates can be explored in more detail by identifying which isoclimates are represented. For example, the novel isoclimates in the Sacramento Valley under the CCSM3-A2, California domain analysis (Figure 11, lower right) consist of precipitation between 269 millimeters (mm) and 1071 mm, minimum temperatures of 0.1°C to 6.6°C (32.2°F to 43.8°F), and maximum temperatures of 39.3°C to 43.1°C (102.7°F to 109.6°F). In the 1971–2000 baseline period, all of these conditions are observed individually, but temperatures this warm were only observed in drier areas (< 269 mm). Thus, this represents a novel combination representing a hot and fairly wet climate, unlike any existing in California in the recent past.

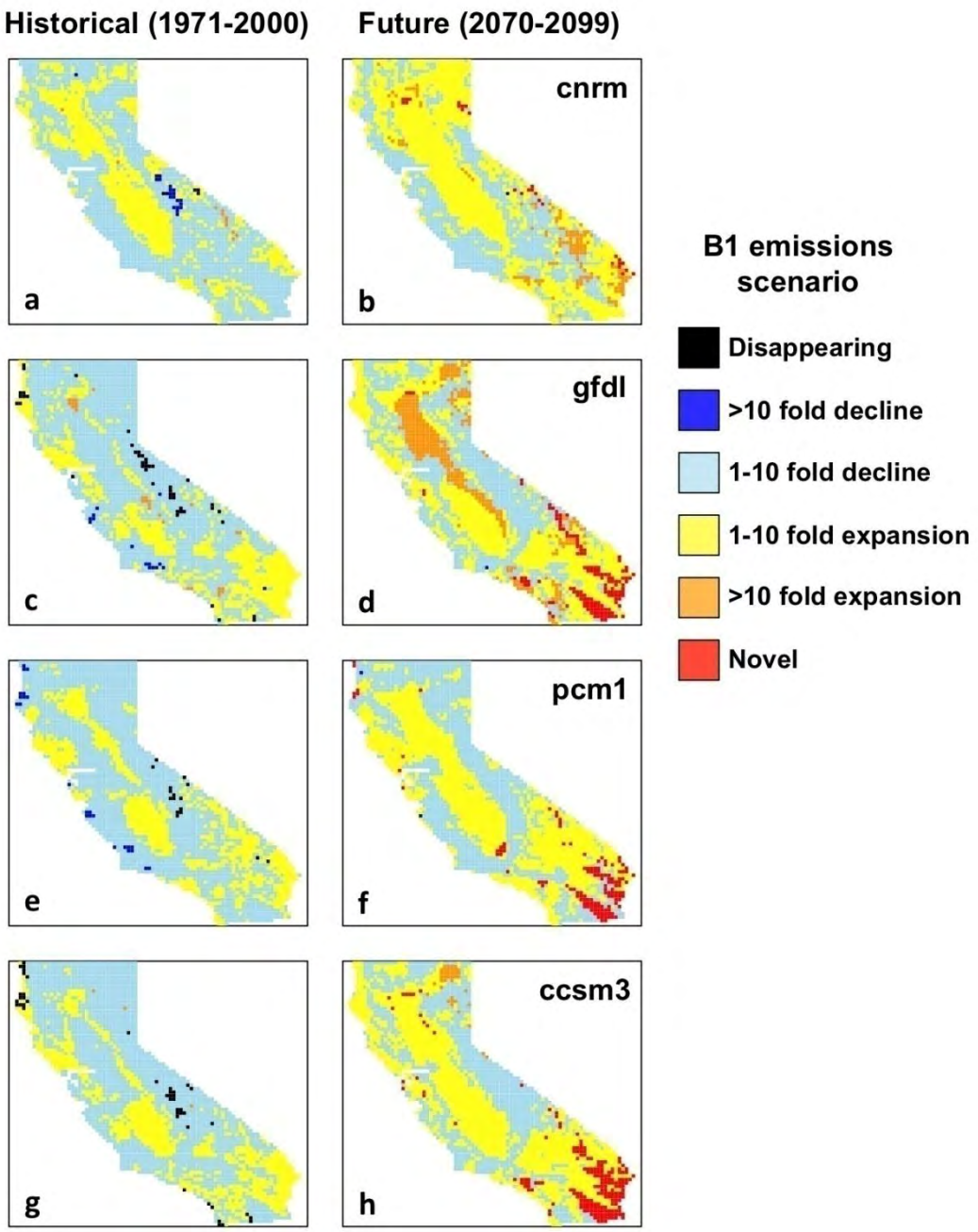

Figure 10. Novel, Disappearing, Expanding, and Shrinking Climates of California, for B1 Emissions Scenario. In each figure, left column shows fate of current climates (1971–2000); right column shows status of projected future climates (2071–2100). Rows represent results for the CNRM, GFDL, PCM1, and CCSM3 general circulation models, downscaled for the 2008 California Climate Change Impacts Assessment Report. Colors: black = disappearing; dark blue = >10-fold reduction; light blue = 1- to 10-fold reduction; yellow = 1- to 10-fold expansion; orange = >10-fold expansion; red = novel climate. For example, in a row, the areas mapped in yellow on left contain climates that will expand up to 10-fold in area, occupying the areas shown in yellow on the right.

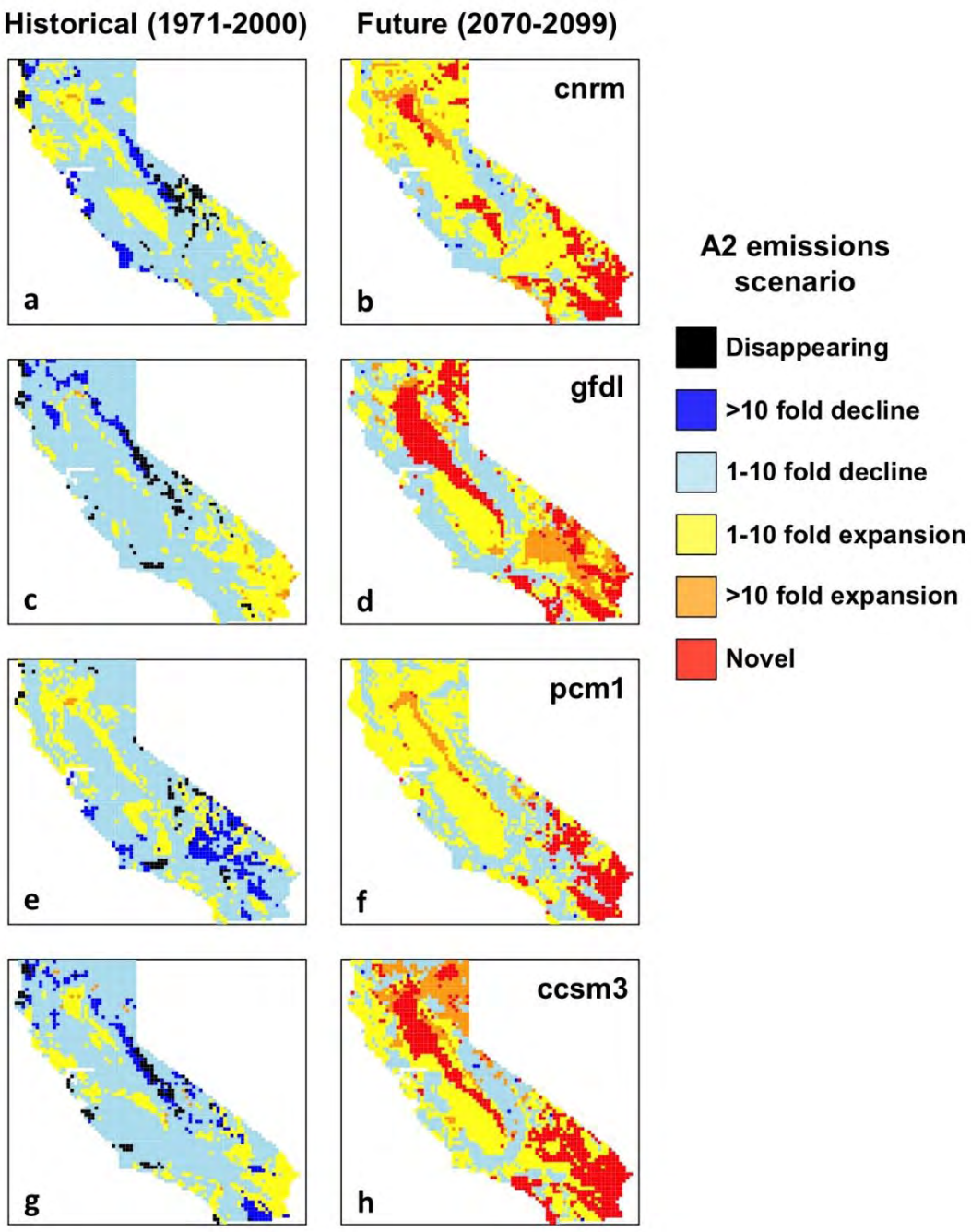

Figure 11. Same as Figure 10, for A2 Emissions Scenario

Discussion

By the end of the twenty-first century, current projections for climate change in California represent marked departures from the range of conditions experienced in the recent past. These changes are primarily driven by increases in temperature, with less marked shifts in precipitation (Cayan et al. 2008). Species distribution modeling projects dramatic shifts for California's endemic flora (Loarie et al. 2008) and reorganization of bird communities (Stralberg et al. 2009) in response to these changes. However, distribution modeling has several drawbacks, including the significant data requirements and the difficulty of summarizing responses for large numbers of species. As a first approximation, the approach used here rests on the assumption that species (or habitats) that occupy particular climatic conditions will be negatively affected if the extent of those climates shrinks, and possibly threatened with local extinction if the climates disappear. Conversely, species that occupy expanding conditions have the potential for increasing range sizes.

The spread of novel climates poses both a statistical and biological challenge. Statistically, projecting species distributions into areas of novel climate requires extrapolation of distribution models beyond the range over which they were parameterized, and extrapolation is always highly uncertain (especially if the models have non-linear terms). Biologically, novel climates may have unpredictable consequences, as analogous conditions do not currently exist within the spatial domain under consideration. Paleoecological evidence suggests that these non-analog climates may lead to non-analog biotic communities (communities not currently observed) (Williams et al. 2001). Under rapid climate change, the shift of isoclimates across the landscape poses an additional challenge, as species must disperse and shift their ranges to track suitable climates. Thus, even for existing isoclimates, biotic responses will be difficult to forecast.

The results presented here (Figures 10 and 11) show broad agreement across GCMs, and much greater change under the A2 emissions scenario compared to B1. Current coastal, California montane, and Great Basin isoclimates generally shrink in extent, while desert and Central Valley isoclimates expand. Novel climates spread into the Sonoran desert, Sacramento Valley, and Great Basin. Presumably these novel climates resemble current conditions in adjoining regions of Arizona and Mexico, though analysis of a broader spatial domain is necessary to determine the location of analogs for these future conditions. The spread of novel climates in the desert regions is broadly similar to the results of Wiens et al. (2011), but the extent is greater here. The two studies differ in the future climate projections used, the time period, and the methods. As a result, it is quite difficult to assess the reasons for different outcomes. At a minimum, the greater area of novel climates shown here probably reflects the analysis of late twenty-first century climates, versus mid-century by Wiens et al. In addition, this study used three climate variables, while Wiens et al. used two composite variables constructed from principal components analysis. I presume that analyses with more variables will be more likely to identify novel climates, as the number of possible isoclimates increases, and the particular combinations found in the past and the future may differ. On the other hand, I believe that the broad bins used here (four historical standard deviations) to discriminate isoclimates would make assessments of

novel climates conservative. A direct comparison of the Wiens et al. probability density approach versus this study's histogram approach would be required to determine which is more conservative in assignment of novel climates.

There are a several implications of this analysis for conservation and land management. If one is concerned with conservation of a particular species, it will be important to determine if the species occupies declining or expanding portions of climate space. The same is true for vegetation types or ecological communities. Those occupying shrinking or disappearing climates, such as high mountains, almost certainly face greater threats than those occupying expanding climates. However, even for species occupying a disappearing climate, extinction is not inevitable, as they may have a broader fundamental niche than is apparent from current distributions, their range may extend beyond areas of disappearing climates (Wiens et al. 2011), or they may be buffered by factors such as edaphic requirements (Damschen et al. 2012) or stable microclimates. Additionally, it is essential to determine how far a climate type is projected to move, in addition to whether it is declining or expanding. If suitable conditions persist, but are far removed from their prior locations, then dispersal barriers may become the primary obstacle to a species survival. In exceptional cases, managed relocation may be an option, but the ecological uncertainties and high cost could be prohibitive (Richardson et al. 2009).

Implications for land managers who are responsible for a reserve, rather than a species or vegetation type, are quite different. Reserves will stay put, as climates and the associated biota shift from underneath our feet (Araujo et al. 2004). Only the largest reserves, and those occupying topographically heterogeneous habitats, may be sufficient to maintain significant overlap between present and future climates over the next century (Loarie et al. 2009; see Section 3 of this paper). Even if the majority of California climates persist somewhere in the state, or in the region, few are likely to persist within individual parks and reserves where they occur now. On the one hand, this means that park management plans focused on maintenance of particular species or vegetation types will need to be realigned to changing conditions. A focus on ecosystem processes and functions, divorced from particular biotic elements, will allow for flexible management targets in the face of change. In addition, it will be critically important to focus increased attention on the species that will be arriving in the future, rather than those that may be lost. The species occupying expanding climates (yellow and orange areas in Figures 10 and 11) may represent the winners under climate change, as suitable areas expand. Conservation of native species in these areas, acting as source populations for future expansion, should be considered as a management priority. Possibly the greatest threat facing many natural areas is the rapid spread of invasive species (native or alien), promoted by high fecundity and long-distance dispersal, that may establish before the arrival of more "desirable" native biota.

The most significant obstacle to translating these analyses for decision-making by managers is the uncertainty arising from the range of future climate scenarios, and the contrasting results that emerge from different analyses (e.g., comparing Ackerly et al. 2010; Wiens et al. 2011: and this study). Variation among GCMs was relatively small in this study, which is encouraging (reading down the columns in Figures 10 and 11). The difference between the lower and higher

emissions scenarios (B1 and A2 here) was primarily in the magnitude of the changes, rather than the pattern. In other words, areas classified as expanding climates under B1 may be novel climates under A2, and under the higher scenario more of the state was classified in the higher 10-fold increase and decrease categories. In contrast, as discussed above, the results from Wiens et al. were quite different in the extent and to a degree the pattern of novel and disappearing climates. The difference in methodology, choice of climate variables, and mid versus late-century future time period likely all contributed to these differences. Resolution of these differences will require that the conservation and climate change community evaluate alternative methods and seek consensus. If this is done, it will be possible to conduct ensemble analyses across a full suite of GCM and emissions scenarios, and provide results that summarizes the pattern, magnitude and degree of uncertainty in the projected changes.

Section 3: Topographic Heterogeneity and the Resilience of California's Protected Areas

The vulnerability of protected areas, and their constituent biota, in the face of climate change will be affected by many factors, including the magnitude of the changes that occur, the size and climatic heterogeneity of the reserves, the intrinsic sensitivity of the species, and the nature of obstacles to range shifts or other adaptive responses, both within reserves and across the broader regional landscape (Klausmeyer et al. 2011). It is generally expected that climatic heterogeneity will enhance resilience, as heterogeneous reserves are likely to harbor more species and genetic diversity, promoting ecological and evolutionary responses, and to facilitate range shifts over shorter distances along climatic gradients within reserves (Ackerly et al. 2010). Due to the basic physics of climate, a broad elevational range and rugged topography will increase climatic heterogeneity, due to elevational lapse rates for temperature, varied solar insolation and cold air pooling at more local scales, orographic rainfall patterns, and rainshadows (Dobrowski 2011). Other factors will be regionally important; for example, cold oceans can generate a strong temperature gradients, fog, and other local climatic variation. This effect is strikingly observed along the California coast, such as the San Francisco Bay Area, where summer maximum temperatures increase as much as 6°C (11°F) in the first 15 km inland from the coastline (based on analysis of PRISM climate data).

The goals of this analysis were:

1. to quantify climatic variability in reserves and protected areas of California, as a measure of the potential for plants and animals to move across these gradients in response to climate change;
2. to quantify the climatic overlap for protected areas, based on the overlap in distributions of historical versus projected future conditions; and
3. to test the relative contribution of reserve size, elevational range, and position relative to the coast as factors contributing to climatic overlap.

Methods

Conservation Units: As a first step, a set of large and spatially contiguous (or near contiguous) areas was identified, which are referred to here as "Conservation Units." These units were identified as follows:

1. Version 1.6 of the California Protected Areas Database (CPAD 1.6) was downloaded from www.calands.org (August 2011). Starting with the SuperUnits database (which has over 14,000 protected areas), all areas of greater than 1000 hectares (ha) were extracted. A few dozen units that appeared more than once under the same name were then combined (these were separated in the database due to differences in accessibility).
2. The areas were then assigned to one of four categories: (a) units that were stored as a single spatial polygon; (b) units that had multiple polygons but all polygons were adjoining, so the entire area was contiguous; (c) units that had non-contiguous polygons with small gaps between them (<2 km), which were considered near-contiguous; and (d) units that were spatially disaggregated with large gaps between different areas. Units in categories a through c were used as is. Those in category d were examine visually, and broken into separate pieces that satisfied one of the first three criteria. In the process, small outlying areas were excluded if they were < 1000 ha.
3. Any units with the word "Lake" or "Reservoir" in their name were plotted along with the "hydro_poly" layer from the Cal Atlas hydrological features database, and units that were > 50 percent water (by visual estimate) were excluded (total of 22). These first three steps resulted in a database of 370 conservation units.
4. Two SuperUnits were too large and dispersed to separate into contiguous units by visual examination: Bureau of Land Management (BLM) (10212 individual polygons covering 6.3 million ha) and the California State Lands Commission (918 polygons covering 176,000 ha). For these, any individual polygon > 1000 ha was extracted and included in the final data set. As a result, adjoining polygons from these SuperUnits were treated separately. This step added an additional 259 units to the database, the largest of which was over 3 million ha.

The resulting database had a total of 629 conservation units, ranging in size from the minimum of 1000 ha to a maximum of 3.1 million ha for a single polygon of BLM lands spanning portions of the Sonoran and Mojave deserts (Figure 12). The total area encompassed is 19.3 million ha, representing 97 percent of the area in the entire CPAD database, and 47 percent of the State of California. The resulting database is available from the author as an Arc format shapefile (CPAD16_CU1k). Six units situated along the coastline were removed from data analysis because they did not overlap any pixels in the climate data sets, resulting in a final sample size for analysis of 623.

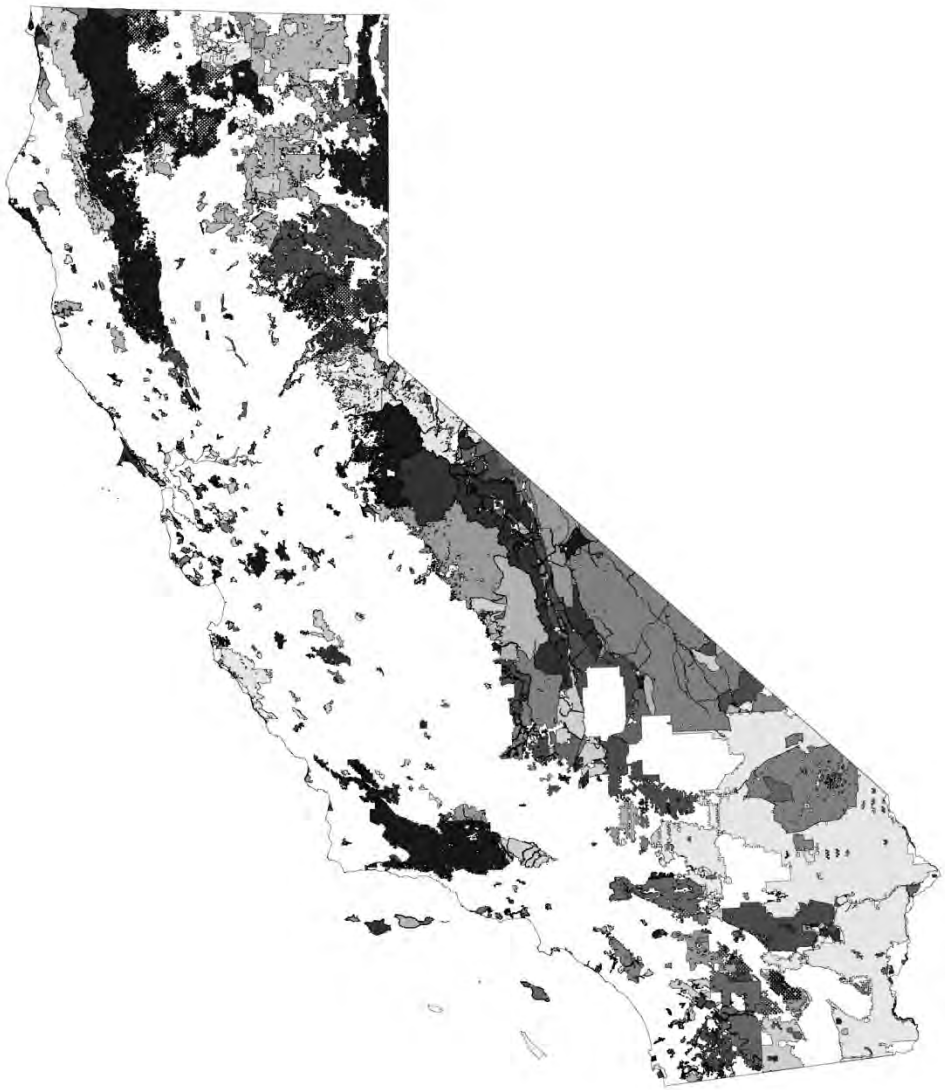

Figure 12. Conservation Units Derived from the California Protected Areas Database v.1.6. Units Were Defined as Contiguous Areas of > 1000 ha (see text for details). Gray scale is arbitrary, to highlight boundaries between adjacent reserves.

Climatic Variability: Six climate variables derived from the PRISM interpolated climate data set (Daly et al. 2008) were used for this analysis, using the 30 arc second (~800 m) 1971–2000 norms (Figure 13a–f):

1. T_{min} (°C): mean minimum temperature of the coldest month of the year (calculated pixel-wise to account for spatial variation in which month is coldest)
2. T_{max} (°C): mean maximum temperature of the hottest month of the year (also calculated pixel-wise)
3. T_{mean} (°C): mean annual temperature, calculated as the average of monthly mean temperatures
4. T_{seas} (°C): temperature seasonality, calculated as the standard deviation of monthly mean temperatures
5. P_{Ltot} (log mm): log10 of total annual precipitation (log transformation was used due to the extremely skewed distribution of precipitation values across California; see Ackerly et al. 2010)
6. P_{seas} (%): precipitation seasonality, calculated as the coefficient of variation (CV) of monthly precipitation (CV was used instead of standard deviation to account for scaling of variance with mean).

Two geographic layers were also analyzed for each reserve (Figure 13g, h):

1. Digital elevation model (DEM) (m): elevation (from the 30 arc second DEM obtained from PRISM)
2. D2C (km): distance to the coast (calculated with the *dist2Line* function in the R *geosphere* library, Hijmans et al. 2011); for this analysis, the coastline included San Francisco Bay as far as the Carquinez Strait.

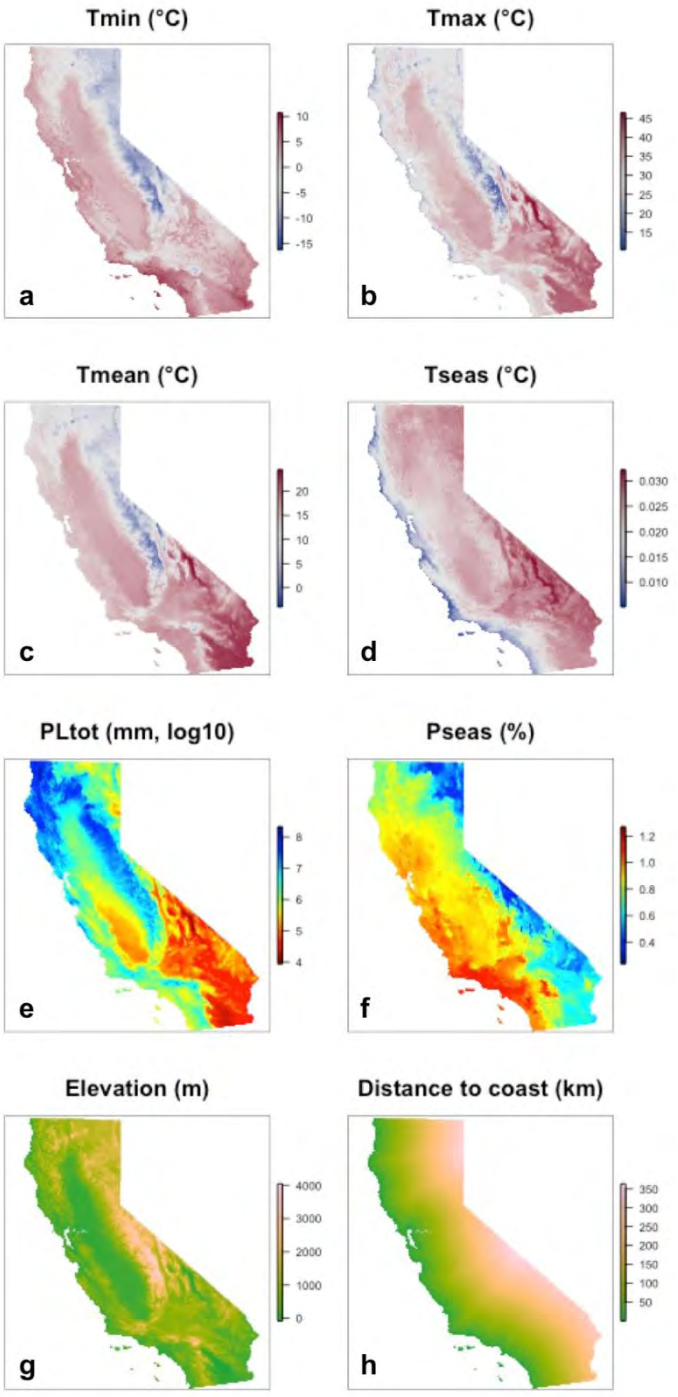

Figure 13. Eight Climate and Topographic Layers Used for Overlay on Conservation Units Database. Mean, standard deviation, and range for each parameter were calculated for each conservation unit. T_{min}: mean monthly minimum temperature; T_{max}: mean monthly maximum temperature; T_{mean}: mean annual temperature; T_{seas}: temperature seasonality, measured as standard deviation of monthly temperatures; P_{Ltot}: total annual precipitation (mm, log10

transformed); P_{seas}: precipitation seasonality, measured as coefficient of variation of monthly precipitation.

ASCII grids for all layers were transformed to Teale Albers projection, and then resampled to a rectangular grid of 800 m pixels (= 64 ha). The polygon(s) for each conservation unit were overlaid on the raster maps of each of the eight climate and geographic variables, and the corresponding values were obtained using the *extract* function in the R *raster* library. Five summary statistics were then calculated for each variable: minimum, maximum, mean, standard deviation, and range, as well as the sample size (number of pixels).

Relationships between reserve size and the range and variability of elevation and the six climate variables were examined visually. It is important to recognize that the climate interpolation algorithms used by PRISM, like other spatial interpolation methods, are driven primarily by elevational effects, with secondary incorporation of regional effects such as maritime influences, rain shadows, etc. (see Daly et al. 2000, 2008). As a result, strong relationships will necessarily arise between elevational range and climatic range, especially for temperature and precipitation. However, to the extent that the interpolation algorithms accurately capture the true spatial patterns in climate, these relationships are useful in considering the climatic heterogeneity of conservation units in relation to their size and topography.

Climate Overlap: The analysis of climatic overlap was based on the 7.5 arc min climate layers from the 2008 California Climate Change Impacts Assessment Report. Individual pixels at this scale are approximately 17,000 ha, so these analyses were necessarily very approximate for the small reserves in the conservation units database. The elevational range spanned by a reserve was calculated based on the 7.5 arc min DEM, for consistency among climate and topography values. Reserve size was measured as the number of pixels extracted from the climate layers, so that small reserves all collapsed to a value of 1. Following the algorithms above (Section 2), climatic conditions in each reserve were assigned to isoclimates, and the relative frequency of each isoclimate was tabulated under historical and future conditions. Analyses presented here are for the A2 emissions scenario and the CCSM3 GCM results only. The overlap of the climate distributions in a reserve was calculated as 1 minus the Bray-Curtis dissimilarity value, comparing the two isoclimate tables and using the frequency of each isoclimate as the analog of species abundance. This ranges from 0 when there is no overlap (all isoclimates present in one table are absent in the other) to 1 for identical distributions.

Multiple regression was used to evaluate the relationship of climatic overlap to reserve size, elevational range, and distance to coast. Akaike Information Criterion (AIC) was used to evaluate alternative linear models to find the best set of predictors that explain variation in climate overlap.

Results

The range of elevations spanned by each conservation unit is strongly correlated with unit area, (Figure 14). Note that this relationship is roughly log-linear, with reserve size log-transformed. This positive relationship would generally be expected in a heterogeneous landscape, but also

reflects the distribution of protected areas in California. For example, if there were large conservation units in the Central Valley, then it would be possible to have large reserves with low relief (lower right corner), but these are not observed in the California conservation lands network. All units above 50,000 ha are located in mountainous areas of the Sierra Nevada, deserts and Coast Ranges, and have elevational ranges of at least 1000 m.

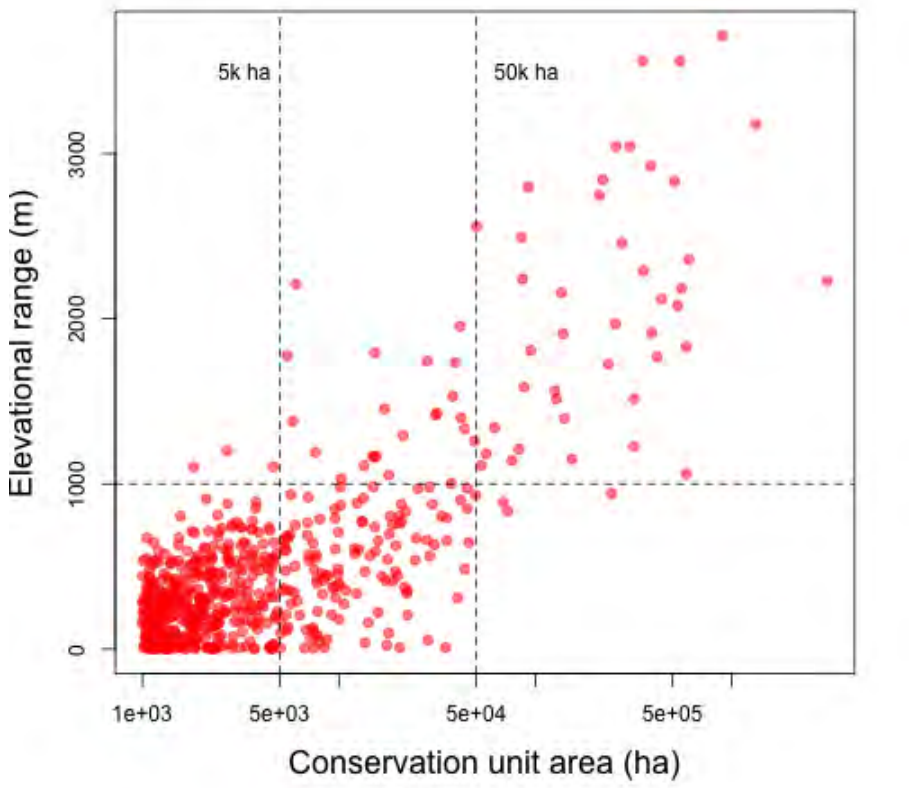

Figure 14. Elevational Range vs. Area for 623 Conservation Units Shown in Figure 3.1. See the text for a discussion of thresholds at the 1000 m elevation range, and 5000 and 50,000 ha area. A transparent color was used to highlight the large number of overlapping points in the lower left quadrant.

The ranges of T_{min}, T_{max}, and T_{mean} all rise in direct relationship with the range of elevations (reflecting the primary role of elevation in the climate interpolation algorithms, as noted above) (see Figure 15). The slope for T_{max} is steeper than that for T_{min}, and T_{mean} is intermediate. The T_{max} slope of 7.3°C per 1000 m approximates the elevational lapse rate for temperature. The range of T_{seas} also increases with elevational range, though with considerable scatter. The range of T_{seas} is greater in reserves near the coast (results not shown), reflecting the steep coastal-inland gradient in the first 50 km from the ocean (Figure 13d). Precipitation and precipitation seasonality also increase with the elevational range of conservation units. Elevational and climatic range were

strongly correlated with the standard deviations for the respective variables (r^2 from 0.93 to 0.97). While range values will reflect the effects of occasional outlying values, they are presented here as they are easier to interpret than standard deviations.

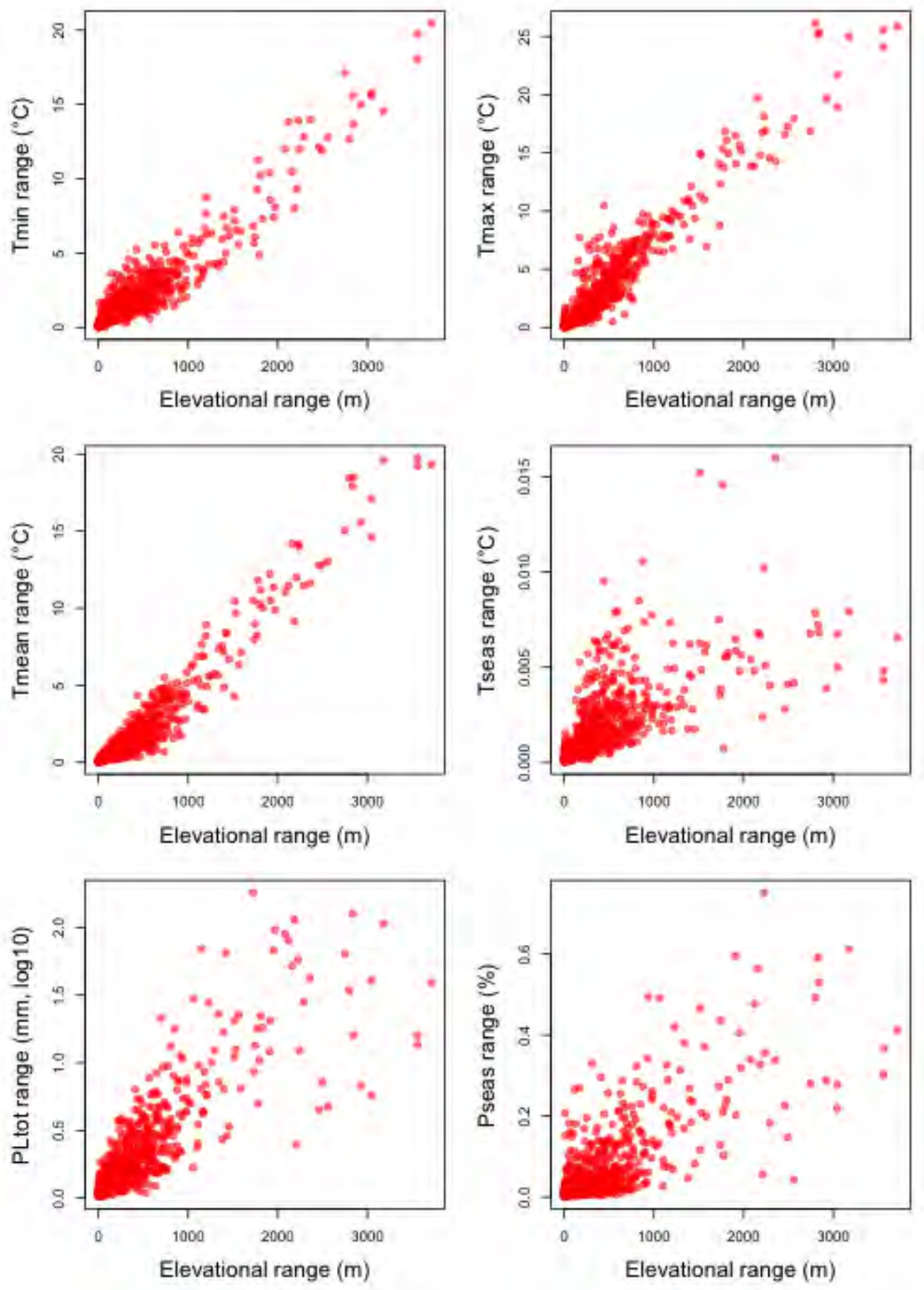

Figure 15. The Range of Environmental Conditions in Conservation Units, Relative to their Size and Elevational Range

Multiple regression analysis demonstrated that climate overlap increased in larger conservation units, in units spanning a greater elevational range, and in units closer to the ocean (Figure 16); all of these effects were included in the best-fitting model (lowest AIC), indicating that they make independent contributions while accounting for the other factors. The effect of distance to the coast is presumably due to both the steep spatial gradients near the coast and the reduced magnitude of change (Figure 8). A reduced model without reserve size had only slightly lower support (AIC 2.5 units higher), demonstrating that most of the effect of reserve size is captured by elevational range, with only a very small additional explanatory role for size per se. The overall R^2 of the full model was only 16.2 percent, indicating substantial unexplained variability. Most of this variance was at the lower end of reserve sizes, and may reflect stochastic effects of the small number of pixels and the effects of converting continuous variables to discrete bins for classification of isoclimates.

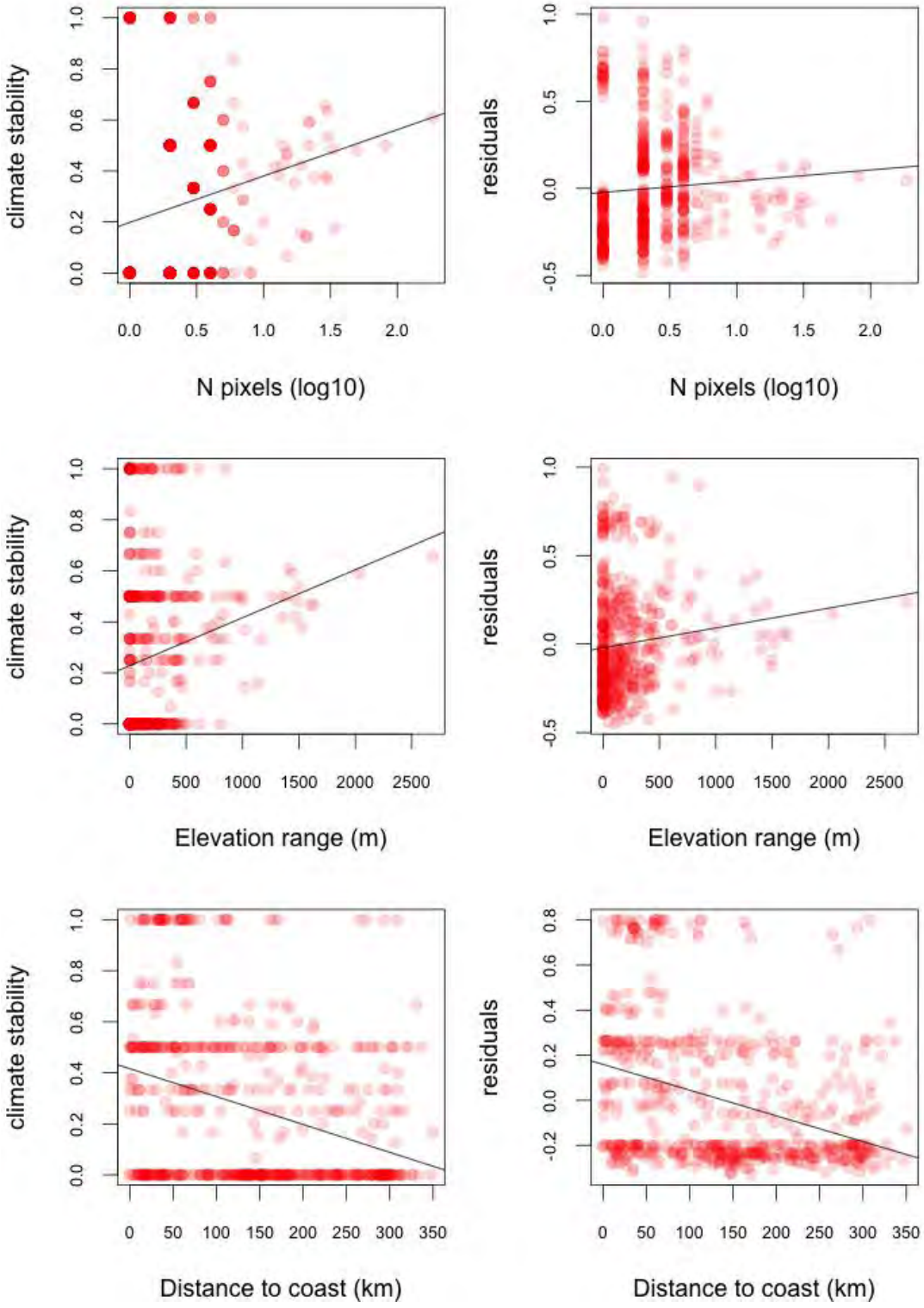
climate stability
0.0
0.2
0.4
0.6
0.8
1.0
0.0
0.5
1.0
1.5
2.0
N pixels (log10)
residuals
-0.5
0.0
0.5
1.0
0.0
0.5
1.0
1.5
2.0
N pixels (log10)
climate stability
0.0
0.2
0.4
0.6
0.8
1.0
0
500
1000
1500
2000
2500
Elevation range (m)
residuals
-0.5
0.0
0.5
1.0
0
500
1000
1500
2000
2500
Elevation range (m)
climate stability
0.0
0.2
0.4
0.6
0.8
1.0
0
50
100
150
200
250
300
350
Distance to coast (km)
residuals
-0.2
0.0
0.2
0.4
0.6
0.8
0
50
100
150
200
250
300
350
Distance to coast (km)

Figure 16. Climate Overlap of Conservation Units, Relative to their Size, Elevational Range, and Minimum Distance to the Ocean. Left panels: pairwise scatterplots. Right panels: residuals of climate overlap after accounting for the other two factors.

Discussion

This analysis provides a quantitative view of the importance of reserve size and elevational range to enhance the climatic variability of protected areas. The overall patterns are not surprising and follow directly from the elevational lapse rates on temperature and orographic precipitation patterns. The analysis of climate variability and overlap has two primary implications for conservation.

First, environmental heterogeneity enhances biological diversity, over and above the direct effects of reserve area per se. This positive effect of heterogeneity has been clearly demonstrated in the case of species diversity (Kreft and Jetz 2007), and is also observed for genetic diversity within species (e.g., Sork et al. 2010). Increased diversity provides insurance in the face of climate change, as it increases the likelihood that some genotypes and species will occur in conservation areas that can survive, and even thrive, under future conditions. However, the persistence of taxa also depends on the persistence of suitable climates. Thus, the second important role of climatic heterogeneity is to increase the overlap between historical and future conditions, indicating that some of the climates that have been observed in the past will persist within the boundaries of a conservation area. As there should be few barriers to dispersal within a protected area, there will be greater potential for species to track shifting climates within reserves, without having to cross over areas that have been developed.

The results in Figure 16 demonstrate that an elevational range of at least 1000 m ensures a fairly high overlap between historical and future climates. Note that in this analysis, the elevational range was calculated from the 7.5 arc min (12 km) DEM, to correspond with the climate layers, so the full climatic range at finer spatial scales will be underestimated (each pixel will have both lower and higher locations within it, so there will be a larger range overall). It will be valuable to repeat this analysis using downscaled historical and future climate layers at 30 arc sec resolution, and using the newly available 270 m downscaled climate layers that account for smaller-scale topographic effects (Flint and Flint 2012). At a state wide level, the latter are computationally difficult, but they will be critically important in localized analyses for individual reserves.

Setting aside these issues of scale, the direct relationship between elevational range and temperature range (Figure 15) allows for some simple guidelines regarding climatic overlap in the face of climate change. Elevational lapse rates range from 4°C to 7°C per 1000 m, for minimum versus maximum temperatures and in different regions due to regional climate effects. Thus, if twenty-first century climate change entails, for example, a 3°C (5.4°F) warming, then a range of at least 400–700 m is necessary to ensure overlap between the warmest temperatures in a reserve historically and the coldest temperatures in the future (see a similar analysis on the San Francisco Bay Area, Ackerly et al. 2010). For conservation purposes, the overlap must be substantial to ensure the persistence of significant area of suitable habitats.

Thus a minimum elevational range of 1000 m may be necessary to provide a wide range of climatic conditions in the face of projected levels of climate change. In the California protected area network, a range of 1000 m is rarely observed in reserves of less than 5000 ha, and is only ensured in areas of more than 50000 ha (Figure 14). Conservation units with range exceeding 1000 m are highlighted in red in Figure 17.

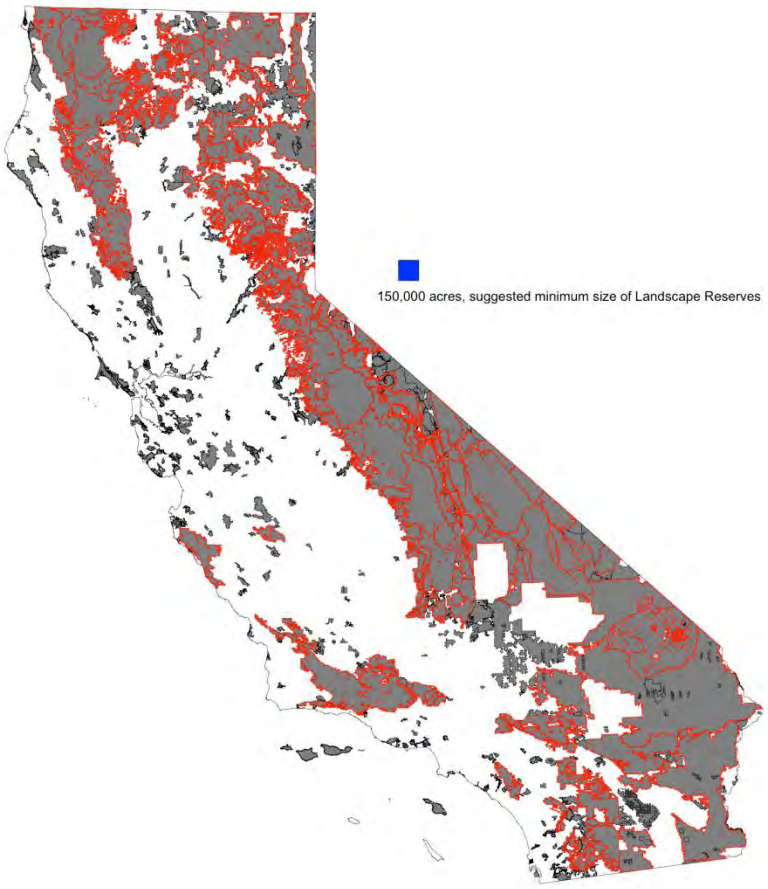

Figure 17. Conservation Units Used in this Analysis; Areas with an Elevational Range of > 1000 m Are Outlined in Red. The blue box shows the size of 150,000 acres (= 61,000 ha), the minimum size for Landscape Reserves proposed in the 2009 California Climate Change Adaptation Strategy.

It is important to recognize that the current analysis relies on administrative definitions of protected areas. In many areas, especially in the Sierra Nevada, protected areas share boundaries such that the effective size from a conservation and biological perspective is much larger than the size of an individual park or administrative unit. In the face of climate change, it will be increasingly important to look at the collective conservation status of a landscape, and define conservation units based on contiguous areas that include multiple administrative units. Construction of a GIS database of contiguous protected areas would be a valuable step for to aid

future analyses. Additionally, the conservation value of lands that are not formally protected may be quite high, and can be protected and enhanced with appropriate management strategies. The 2009 California Climate Change Adaptation Strategy (California Natural Resources Agency, 2009) proposed the creation of Landscape Reserves, large and heterogeneous landscapes that may include a mix of protected areas and working lands, to enhance biodiversity conservation in the face of climate change. A minimum size of 150,000 acres (= 61,000 ha) was proposed as a guideline for design of these reserves; this corresponds to an area one-sixth the size of Yosemite National Park (see the scale box in Figure 16). The results presented here show that reserves of this size, at least in the current network of protected areas, will all have elevational ranges of at least 1000 m, with some exceeding 3000 m. This suggests that the proposed size is in the appropriate range to achieve a high degree of climate overlap between present and future conditions.

The conservation of large and heterogeneous areas is only one of the potential conservation strategies in the face of climate change. Climatic gap analyses can identify climate types not represented in a current protected area network, which can used to prioritize acquisition of "missing assets," even in the absence of detailed biotic data (Davison et al. 2012). Mapping of novel and disappearing climates in relation to protected reserves can help to identify alternative management strategies in the face of climate change (Wiens et al. 2011). Within local areas, recent research has focused on the importance of small scale climatic variation on topographic gradients, which may generate significant climatic variability and climatic overlap even in smaller reserves (Luoto and Heikkinen 2008; Randin et al. 2009; Ackerly et al. 2010; Scherrer and Körner 2011). Topoclimate variation arises due to factors such as solar insolation effects on north- versus south-facing slopes and cold air pooling in low-lying areas, and does not depend on a large absolute range in elevation per se. Much of California's plant diversity is also dependent on special soils, and plant communities on unusual substrates, such as serpentines, may be buffered from climate change impacts due to restricted colonization by potential competitors (Damschen et al. 2012). More intensive strategies, including fire and invasive species management, and active efforts to establish new taxa that will be suited to future conditions, may also play a critical role in biodiversity conservation in small and large reserves.

Conclusions

The analyses presented here illustrate several approaches to evaluate and quantify aspects of climate change that are of direct relevance to biological impacts, without requiring detailed input on species distributions, physiology, or other parameters. Such analyses have the potential to be broadly useful for resource managers, and others interested in projecting the impacts of climate change on biological systems. On the other hand, the utility of the methods also highlights their limitations, as they are parameterized in general terms, and not informed by the biology of a particular species or system. Section 1 examines shifts in freezing isoclines, as freezing represents a particular climatic threshold that impacts many plant and animal species. The goal of this analysis is to highlight the relaxation of cold stress, as opposed to increased heat or drought stress, as a factor that may lead to shifts in species distributions and changes in

ecological communities (and in the location of agricultural activities). These analyses could be refined for particular systems, based on knowledge of physiological tolerances. This may include counterintuitive effects such as the potential for increased cold damage caused by late spring or early fall frosts, if warming temperatures reduce cold hardiness.

The second section evaluates shifts in the area occupied by different isoclimates, and the distribution of disappearing and novel climates, in California. These analyses provide a framework for considering a range of management challenges and strategies in the face of changing conditions. Section 3 extends this analysis to examine the degree of climatic overlap between historical and future climates in protected areas of California. As with all climate change assessments, these analyses present uncertainties due to differences in future scenarios, methodologies, data sources, and spatial and temporal scale of analysis. The most valuable application of these results may be for scenario-building exercises, asking what management strategies should be employed under different hypothetical futures, rather than seeking projections of what is actually expected to occur. Past experience has proven time and again that surprises are inevitable. The current effort to project biotic responses to climate change is unprecedented in scope, and the repeated refrain that there is great uncertainty in future projections may in the end be the most important result to incorporate into decision-making today.

References

Ackerly, D. D., Loarie, S. R., Cornwell, W. K., Weiss, S. B., Hamilton, H., Branciforte, R., and Kraft, N. J. B. (2010) The geography of climate change: Implications for conservation biogeography. *Diversity and Distributions* 16, 476–487.

Ackerly, D. D., Ryals, R. A., Cornwell, W. K., Loarie, S. R., Veloz, S., Higgason, K. D., Silver, W. L., and Dawson, T. E. (2012) Potential Impacts of Climate Change on Biodiversity and Ecosystem Services in the San Francisco Bay Area. California Energy Commission. Publication number CEC-500-2012-037, Sacramento, California.

Allen, C. D., Macalady, A. K., Chenchouni, H., Bachelet, D., McDowell, N., Vennetier, M., Kitzberger, T., Rigling, A., Breshears, D. D., Hogg, E. H., Gonzalez, P., Fensham, R., Zhang, Z., Castro, J., Demidova, N., Lim, J.-H., Allard, G., Running, S. W., Semerci, A., and Cobb, N. (2010) A global overview of drought and heat-induced tree mortality reveals emerging climate change risks for forests. *Forest Ecology and Management* 259, 660–684.

Araujo, M. B., Cabeza, M., Thuiller, W., Hannah, L., and Williams, P. H. (2004) Would climate change drive species out of reserves? An assessment of existing reserve-selection methods. *Global Change Biology* 10, 1618–1626.

Barnosky, A. (2009) Heatstroke: Nature in an age of global warming. Island Press, Washington, D.C.

Burrows, M. T., Schoeman, D. S., Buckley, L. B., Moore, P., Poloczanska, E. S., Brander, K. M., Brown, C., Bruno, J. F., Duarte, C. M., Halpern, B. S., Holding, J., Kappel, C. V., Kiessling, W., O'Connor, M. I., Pandolfi, J. M., Parmesan, C., Schwing, F. B., Sydeman, W. J., and Richardson, A. J. (2011) The pace of shifting climate in marine and terrestrial ecosystems. *Science* (New York, N.Y.), 334, 652–655.

California Natural Resources Agency (2009) 2009 California Climate Adaptation Strategy, Sacramento, California.

Cayan, D. R., Maurer, E. P., Dettinger, M. D., Tyree, M., and Hayhoe, K. (2008) Climate change scenarios for the California region. *Climatic Change* 87, S21–S42.

Daly, C., Gibson, W. P., Hannaway, D., and Taylor, G. (2000) High-quality spatial climate data sets for the United States and beyond. *Transactions of the American Society of Agricultural Engineers* 43, 1957–1962.

Daly, C., Halbleib, M., Smith, J. I., Gibson, W. P., Doggett, M. K., Taylor, G. H., Curtis, J., and Pasteris, P. P. (2008) Physiographically sensitive mapping of climatological temperature and precipitation across the conterminous United States. *International Journal of Climatology* 28, 2031–2064.

Damschen, E. I., Harrison, S., Ackerly, D. D., Going, B. M., and Anacker, B. L. (2012) Endemic plants on serpentine soils: Early victims or hardy survivors of climate change. In Review.

Davis, S. D., Pratt, B. R., Ewers, F., and Jacobsen, A. L. (2007) Freezing tolerance impacts chaparral species distributions in the Santa Monica Mountains. In *Flora and Ecology of the Santa Monica Mountains* (D. A. Knapp, eds.) 159–172.

Davis, S. D., Sperry, J. S., and Hacke, U. G. (1999) The relationship between xylem conduit diameter and cavitation caused by freezing. *Amer J Bot* 86, 1367–1372.

Davison, J. E., Graumlich, L. J., Rowland, E. L., Pederson, G. T., and Breshears, D. D. (2012) Leveraging modern climatology to increase adaptive capacity across protected area networks. *Global Environmental Change* 22, 268–274.

Dobrowski, S. Z. (2011) A climatic basis for microrefugia: The influence of terrain on climate. *Global Change Biology* 17, 1022–1035.

Flint, L. E. and Flint, A. L. (2012) Downscaling future climate scenarios to fine scales for hydrologic and ecologic modeling and analysis. *Ecological Processes* 1, 2.

Füssel, H. M. and Klein, R. J. T. (2006) Climate change vulnerability assessments: An evolution of conceptual thinking. *Climatic Change* 75, 301–329.

Glick, P., Stein, B. A., and Edelson, N. A. (2011) *Scanning the conservation horizon: A guide to climate change vulnerability.* National Wildlife Federation, Washington, D.C.

Gu, L., Hanson, P. J., Post, W. M., Kaiser, D. P., Yang, B., Nemani, R., Pallardy, S. G., and Meyers, T. (2008) The 2007 eastern US spring freeze: Increased cold damage in a warming world?. *Bioscience* 58, 253–262.

Hijmans, R. J., and van Etten, J. (2011) raster: Geographic analysis and modeling with raster data. R package version 1.8-31. http://CRAN.R-project.org/package=raster.

Hijmans, R. J., Williams, E., and Vennes, C. (2011) geosphere: Spherical Trigonometry. R package version 1.2-25. http://CRAN.R-project.org/package=geosphere.

Jackson, S. T., and Overpeck, J. T. (2000) Responses of plant populations and communities to environmental changes of the late Quaternary. *Paleobiology* 26, 194–220.

Kalberer, S. R., Wisniewski, M., and Arora, R. (2006) Deacclimation and reacclimation of cold-hardy plants: Current understanding and emerging concepts. *Plant Science* 171, 3–16.

Klausmeyer, K. R., Shaw, M. R., MacKenzie, J. B., and Cameron, D. R. (2011) Landscape-scale indicators of biodiversity's vulnerability to climate change. *Ecosphere* 2, art88.

Kreft, H., and Jetz, W. (2007) Global patterns and determinants of vascular plant diversity. *Proceedings of the National Academy of Sciences* 104, 5925–5930.

Loarie, S. R., Carter, B. E., Hayhoe, K., McMahon, S., Moe, R., Knight, C. A., and Ackerly, D. D. (2008) Climate change and the future of California's endemic flora. *Plos One* 3, e2502.

Loarie, S. R., Duffy, P. B., Hamilton, H., Asner, G. P., Field, C. B., and Ackerly, D. D. (2009) The velocity of climate change. *Nature* 462, 1052–1055.

Luedeling, E., Zhang, M., and Girvetz, E. H. (2009) Climatic Changes Lead to Declining Winter Chill for Fruit and Nut Trees in California during 1950–2099. *Plos One* 4, e6166.

Lundquist, J. D., Pepin, N., and Rochford, C. (2008) Automated algorithm for mapping regions of cold-air pooling in complex terrain. *J. Geophys. Res*, 113, D22107.

Luoto, M., and Heikkinen, R. K. (2008) Disregarding topographical heterogeneity biases species turnover assessments based on bioclimatic models. *Global Change Biology* 14, 483–494.

Olson, D. M., Dinerstein, E., Wikramanayake, E. D., Burgess, N. D., Powell, G. V. N., Underwood, E. C., D'Amico, J. A., Itoua, I., Strand, H. E., Morrison, J. C., Loucks, C. J., Allnutt, T. F., Ricketts, T. H., Kura, Y., Lamoreux, J. F., Wettengel, W. W., Hedao, P., and Kassem, K.R. (2001) Terrestrial ecoregions of the world: A new map of life on earth. *Bioscience* 51, 933–938.

R Development Core Team (2006) R: A language and environment for statistical computing (www.r-project.org). R Foundation for Statistical Computing, Vienna, Austria.

Randin, C. F., Engler, R., Normand, S., Zappa, M., Zimmerman, N. E., Pearman, P. B., Vittoz, P., Thuiller, W., and Guisan, A. (2009) Climate change and plant distribution: Local models predict high-elevation persistence. *Global Change Biology* 15, 1557–1569.

Raupach, M. R., Marland, G., Ciais, P., Le Quere, C., Canadell, J. G., Klepper, G., and Field, C. B. (2007) Global and regional drivers of accelerating CO_2 emissions. *Proceedings of the National Academy of Sciences of the United States of America* 104, 10288–10293.

Richardson, D. M., Hellmann, J. J., McLachlan, J. S., Sax, D. F., Schwartz, M. W., Gonzalez, P., Brennan, E. J., Camacho, A., Root, T. L., Sala, O. E., Schneider, S. H., Ashe, D. M., Clark, J. R., Early, R., Etterson, J. R., Fielder, E. D., Gill, J. L., Minteer, B. A., Polasky, S., Safford, H. D., Thompson, A. R., and Vellend, M. (2009) Multidimensional evaluation of managed relocation. *Proceedings of the National Academy of Sciences of the United States of America* 106, 9721–9724.

Scherrer, D., and Körner, C. (2011) Topographically controlled thermal-habitat differentiation buffers alpine plant diversity against climate warming. *J. Biogeog.* 38, 406–416.

Sork, V. L., Davis, F. W., Westfall, R., Flint, A., Ikegami, M., Wang, H., and Grivet, D. (2010) Gene movement and genetic association with regional climate gradients in California valley oak (Quercus lobata Née) in the face of climate change. *Molecular Ecology* 19, 3806–3823.

Sperry, J. S., and Sullivan, J. E. M. (1992) Xylem embolism in response to freeze-thaw cycles and water stress in ring-porous, diffuse-porous, and conifer species. *Plant Physiology* 100, 605–613.

Stralberg, D., Jongsomjit, D., Howell, C. A., Snyder, M. A., Alexander, J. D., Wiens, J. A., and Root, T. L. (2009) Re-Shuffling of Species with Climate Disruption: A No-Analog Future for California Birds?. *Plos One* 4, e6825–e6825.

Stuart, S. A., Choat, B., Martin, K. C., Holbrook, N. M., and Ball, M.C. (2007) The role of freezing in setting the latitudinal limits of mangrove forests. *The New Phytologist* 173, 57–583.

Thorne, J. H., Morgan, B. J., and Kennedy, J. A. (2008) Vegetation change over sixty years in the Central Sierra Nevada, California, USA. *Madroño* 55, 223–237.

Veloz, S., Williams, J., Lorenz, D., Notaro, M., Vavrus, S., and Vimont, D. (2011) Identifying climatic analogs for Wisconsin under 21st-century climate-change scenarios. *Climatic Change* Online early.

Wiens, J. A., Seavy, N. E., and Jongsomjit, D. (2011) Protected areas in climate space: What will the future bring?. *Biological Conservation* 144, 2119–2125.

Williams, C. D., Shuman, B. N., and Webb, T.I. (2001) Dissimilarity analyses of Late-Quaternary vegetation and climate in eastern North America. *Ecology* 82, 3346–3362.

Williams, J. W., Jackson, S. T., and Kutzbacht, J. E. (2007) Projected distributions of novel and disappearing climates by 2100 AD. *Proceedings of the National Academy of Sciences of the United States of America* 104, 5738–5742.

Williams, S. E., Shoo, L. P., Isaac, J. L., Hoffmann, A. A., and Langham, G. (2008) Towards an integrated framework for assessing the vulnerability of species to climate change. *Plos Biology* 6, 2621–2626.

Willis, K. J., Bennet, K. D., Bhagwat, S. A., and Birks, J. B. (2010) 4 °C and beyond: What did this mean for biodiversity in the past?. *Systematics and Biodiversity* 8, 3–9.

Woodward, F. I. (1987). *Climate and plant distribution.* Cambridge University Press, Cambridge.

Glossary

AIC	Akaike Information Criterion
BLM	Bureau of Land Management
CCSM3	Community Climate System Model
CNRM	Centre National de Recherches Météorologiques
CPAD	California Protected Areas Database
CV	coefficient of variation
DEM	Digital Elevation Model
GCM	General Circulation Model
GFDL	Geophysical Fluid Dynamics Laboratory
GIS	Geographic Information System
IPCC	Intergovernmental Panel on Climate Change
NCAR	National Center for Atmospheric Research
PCA	Principal Components Analysis
PCM	Parallel Climate Model
PRISM	Parameter-elevation Regressions on Independent Slopes Model
Ptot	total monthly precipitation
SED	Standardized Euclidean Distance
Tmin	mean minimum monthly temperature
Tmax	mean maximum monthly temperature

Appendix Figures

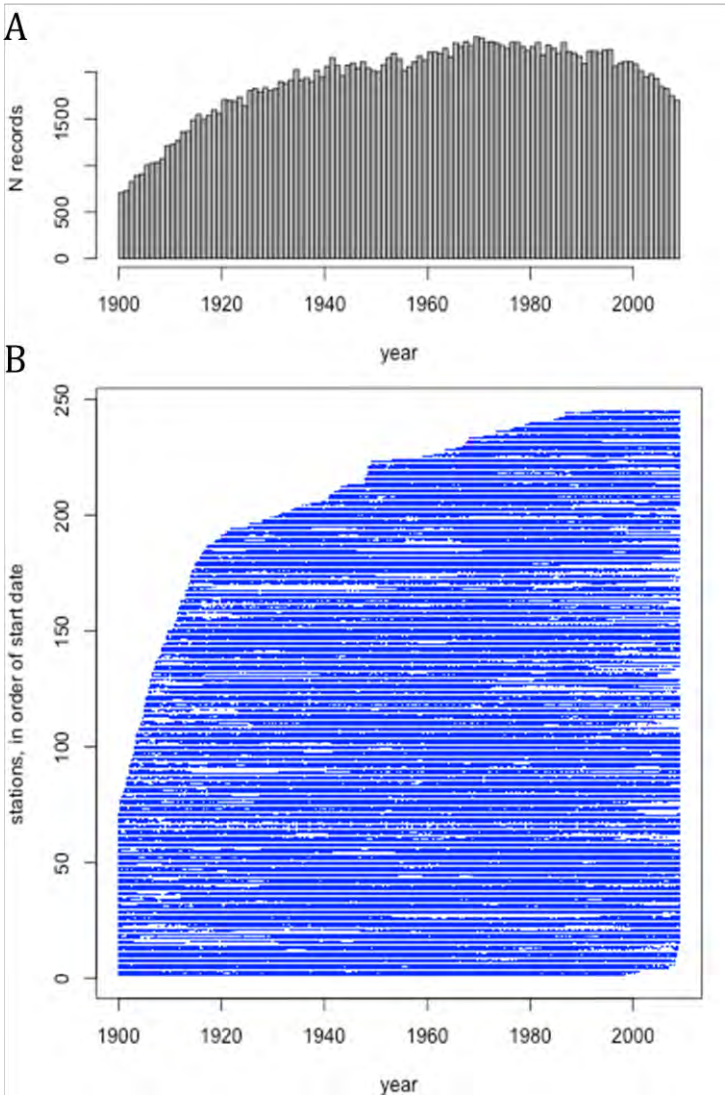

Figure A1. Distribution of Monthly T_{min} Data from the U.S. Historical Climate Network for Stations in the Western States. A: Number of monthly data sets available, by year. B: Time span covered by each station. Each horizontal line represents one station, sorted from bottom to top by start and end dates. Blue dots indicate months with available data.

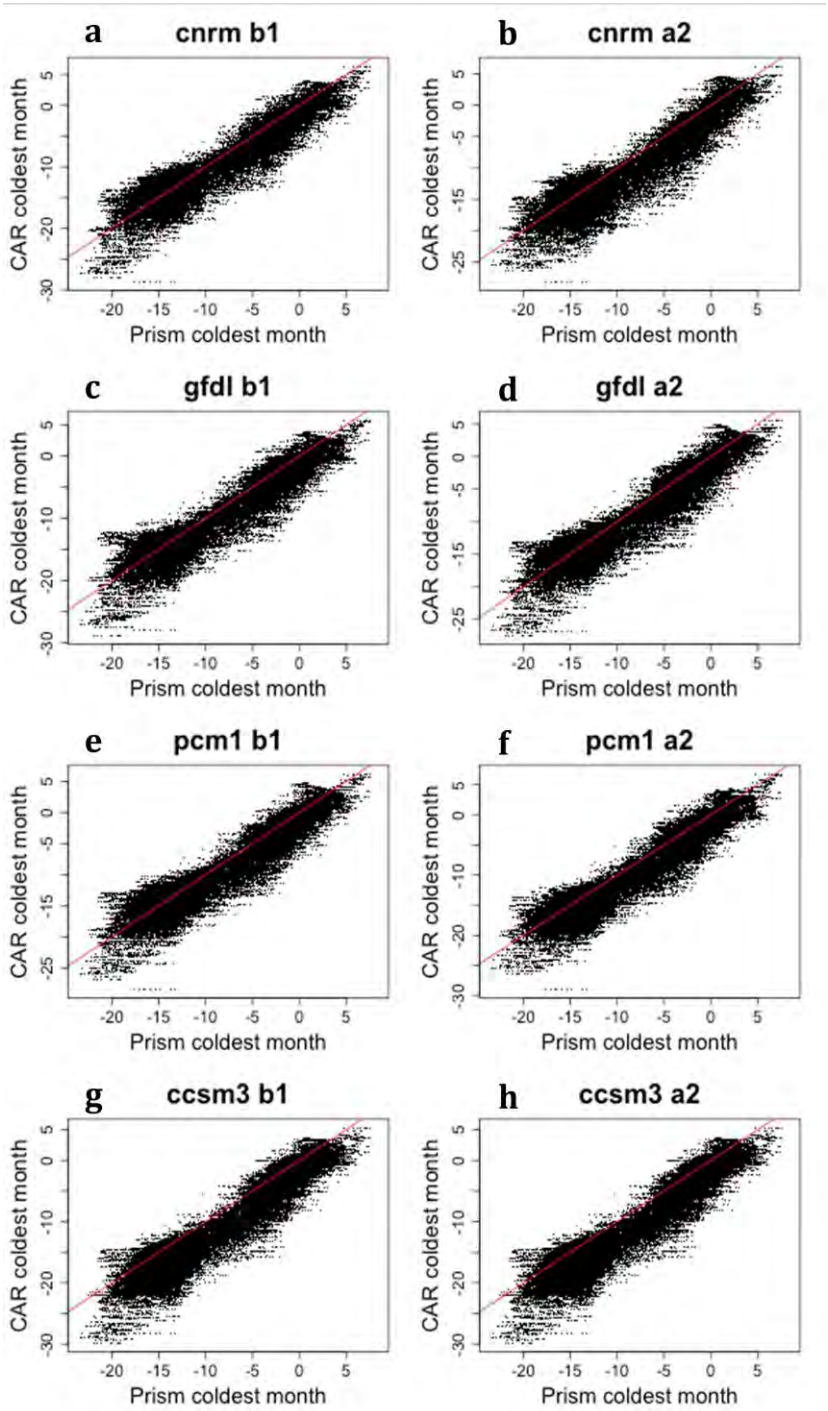

Figure A2. Scatterplot of the Minimum Mean Monthly Temperature for the 1971–2000 Period from PRISM (x-axis) vs. the 2008 California Climate Change Impacts Assessment (CA2008) Downscaled GCM Outputs, for the Same Period. Red lines indicate x = y. Headers on each panel indicate the GCM and emissions scenario used.

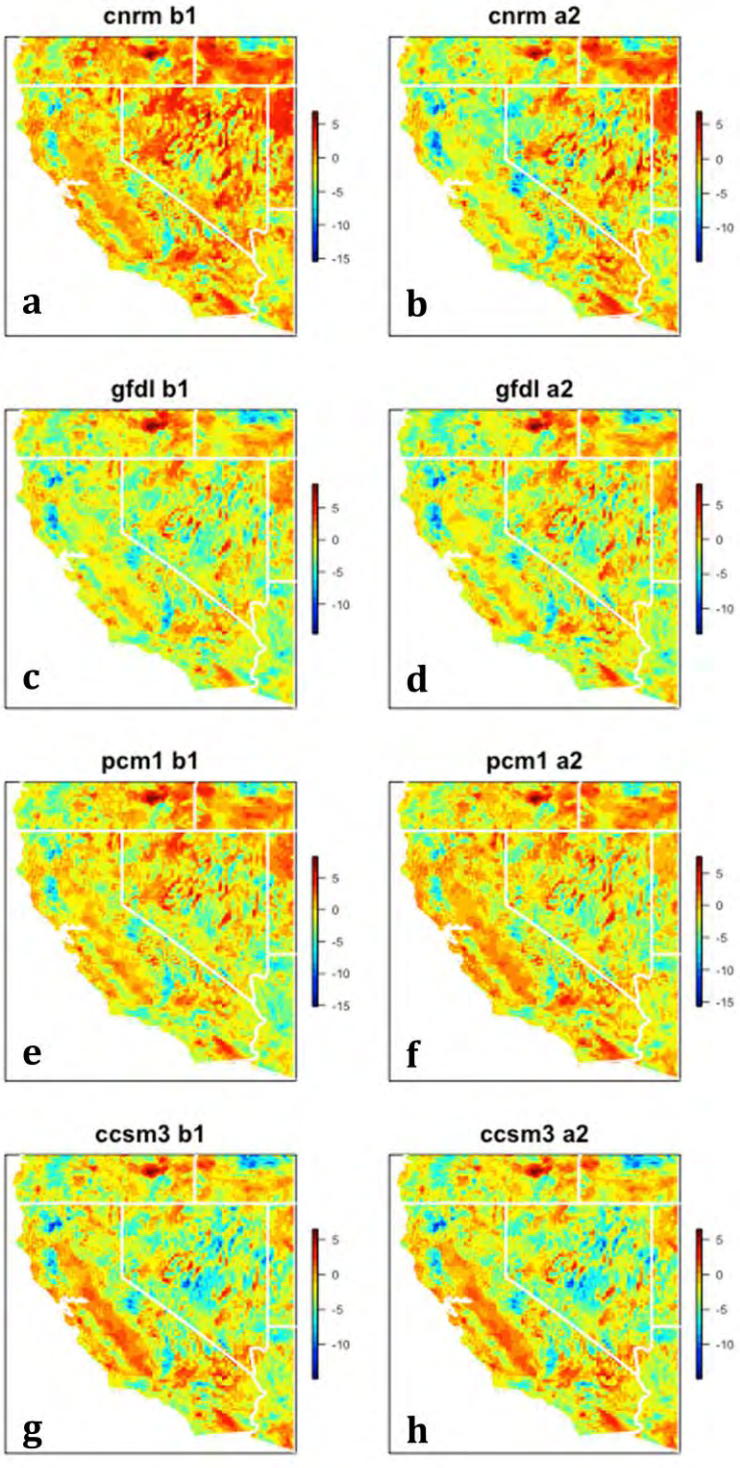

Figure A3. Maps of Deviations in Minimum Mean Monthly Temperature between PRISM and CA2008 Scenarios, as Shown in Figure 1.6. Negative values indicate CA2008 temperatures are colder than the PRISM temperatures.

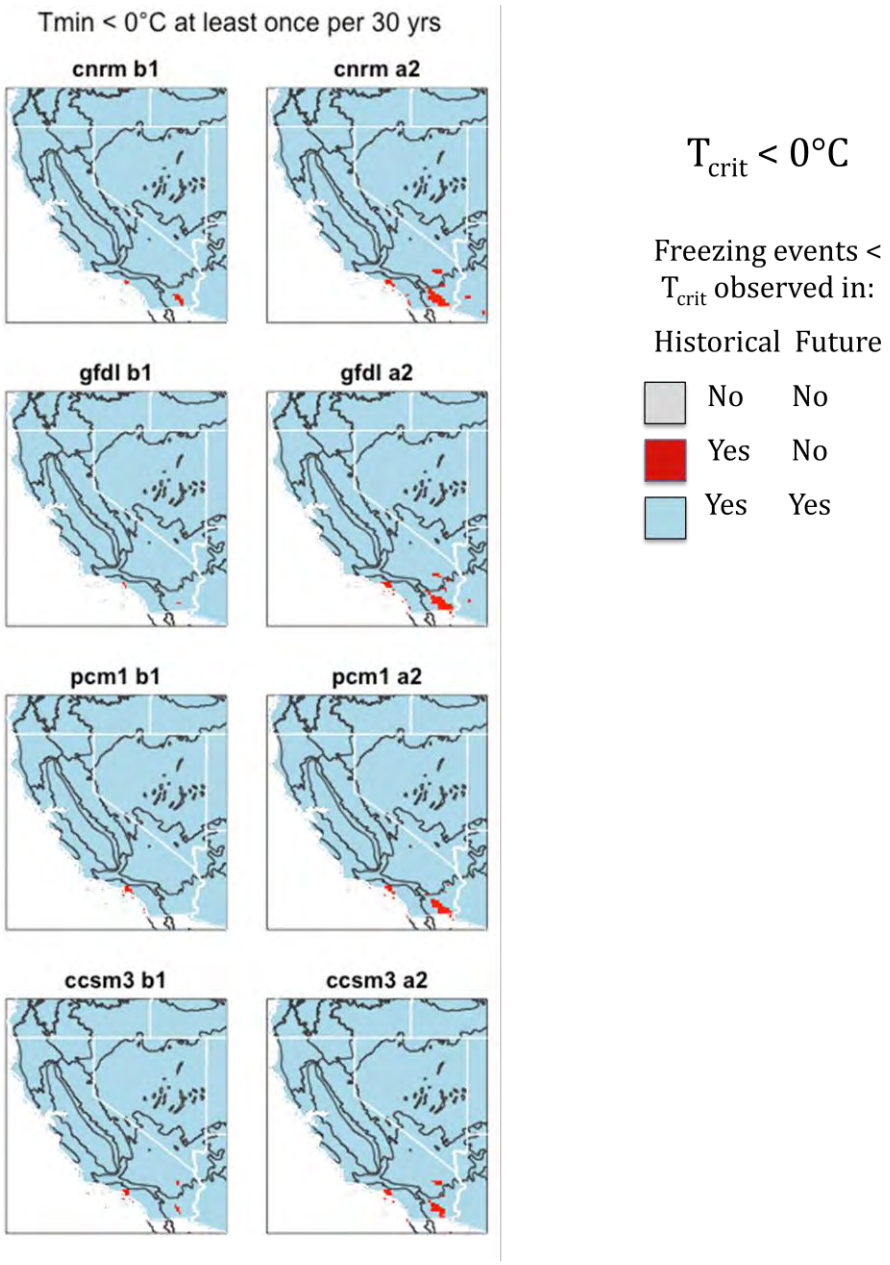

Figures A4–9. Changes in the Distribution of Freeze Events from the 1971–2000 Historical Period to the 2071–2100 Future Projections. Each map corresponds to a different future climate scenario from the CA2008 downscaled projections, with the GCM and emissions scenario noted above. Dark lines show ecoregions (see Figure 2). Blue areas have experienced a freeze < the indicated T_{crit} values in the past, and are projected to continue to experience these events in the future. Red areas have experienced these in the past, but are not projected to experience these in the future. Green are areas that have not experienced a freeze at this temperature in the past, and will not in the future either. A4: T_{crit} < 0°C experienced at least once in the 30-year period. A5: T_{crit} < 0°C experienced at least once per year, on average, during the 30-year period. A6: T_{crit} < -5°C experienced at least once in the 30-year period. A7: T_{crit} < -5°C experienced at least once per year,

on average, during the 30-year period. A8: T_{crit} < -10°C experienced at least once in the 30-year period. A9: T_{crit} < -10°C experienced at least once per year, on average, during the 30-year period.

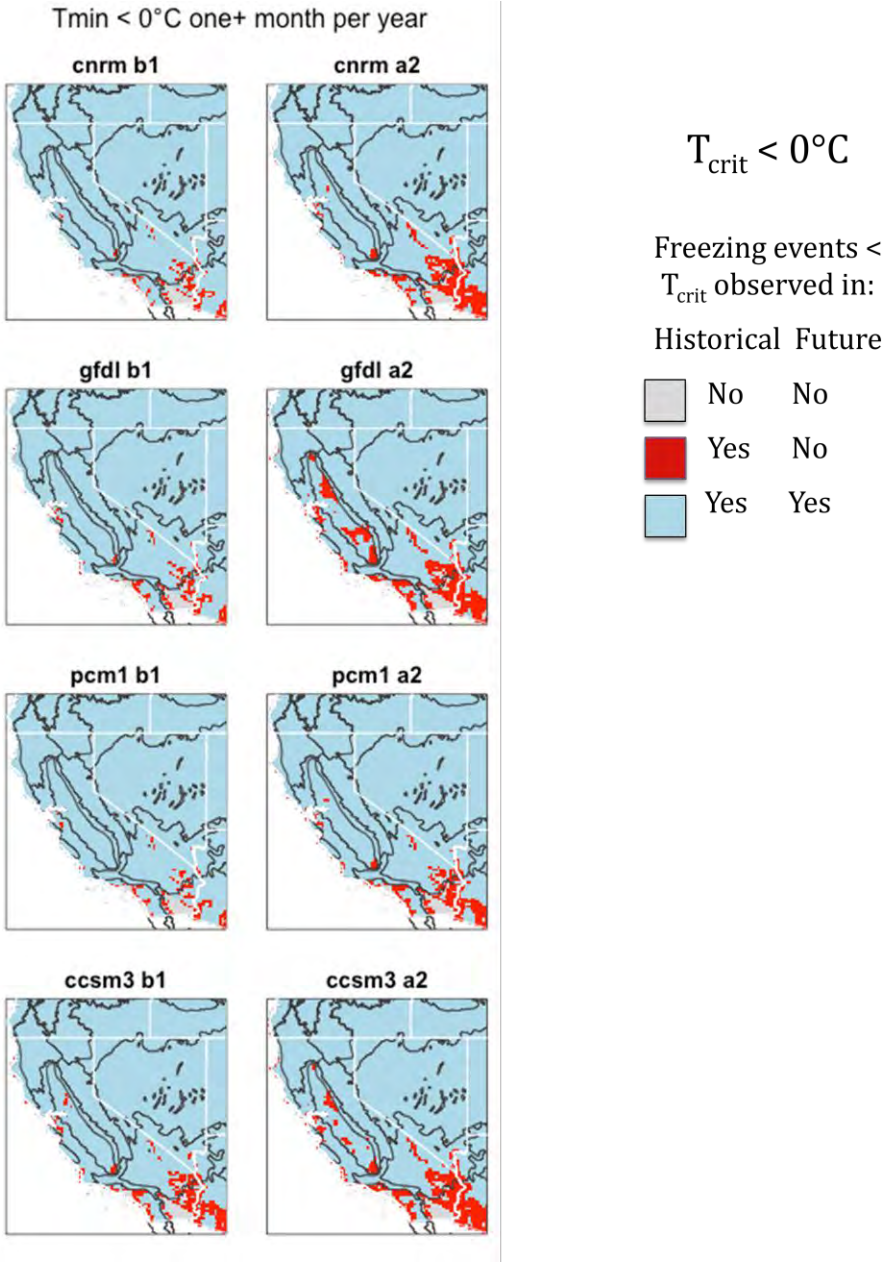

Figure A5. T_{crit} < 0°C Experienced at Least Once per Year, on Average, during the 30-year Period (see the full description above)

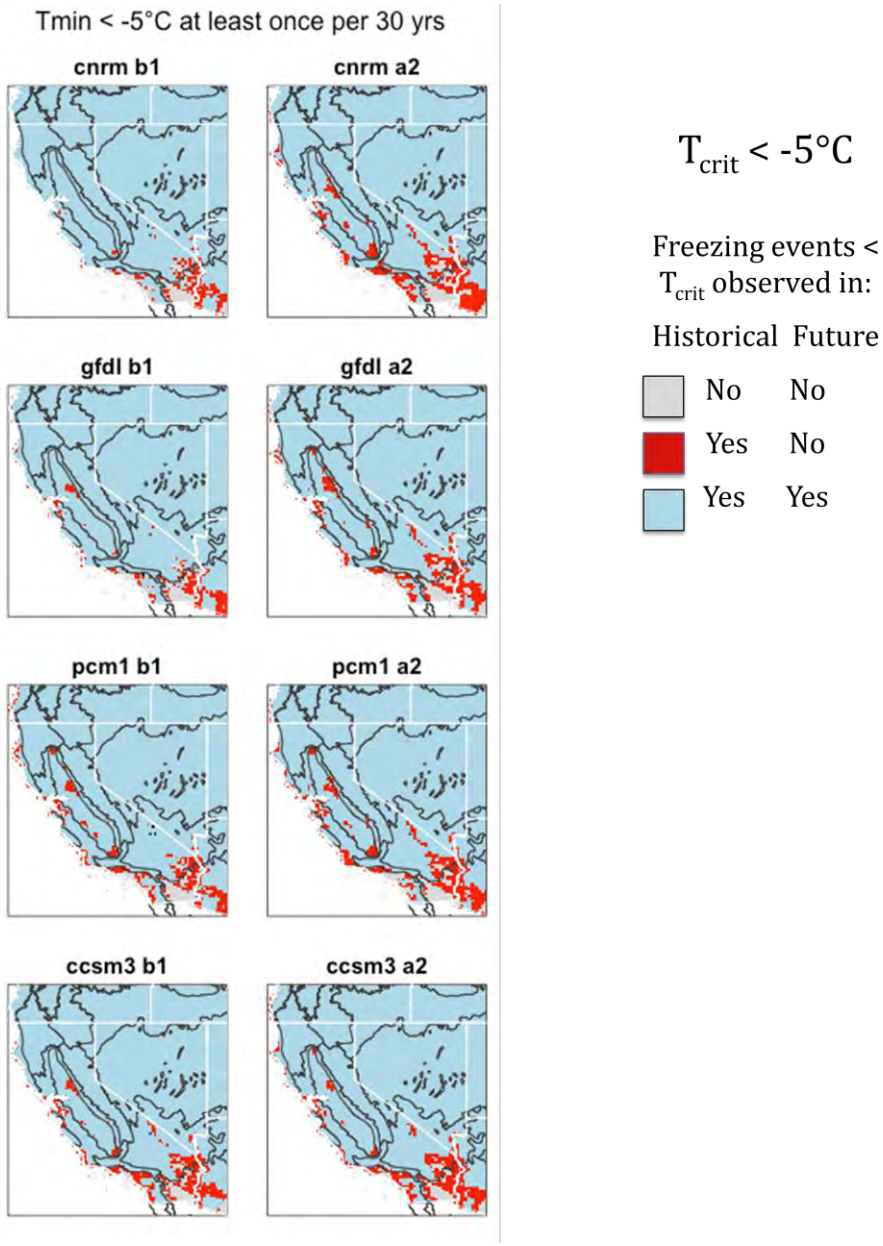

Figure A6. T_{crit} < -5°C Experienced at Least Once in the 30-year Period (see the full description above)

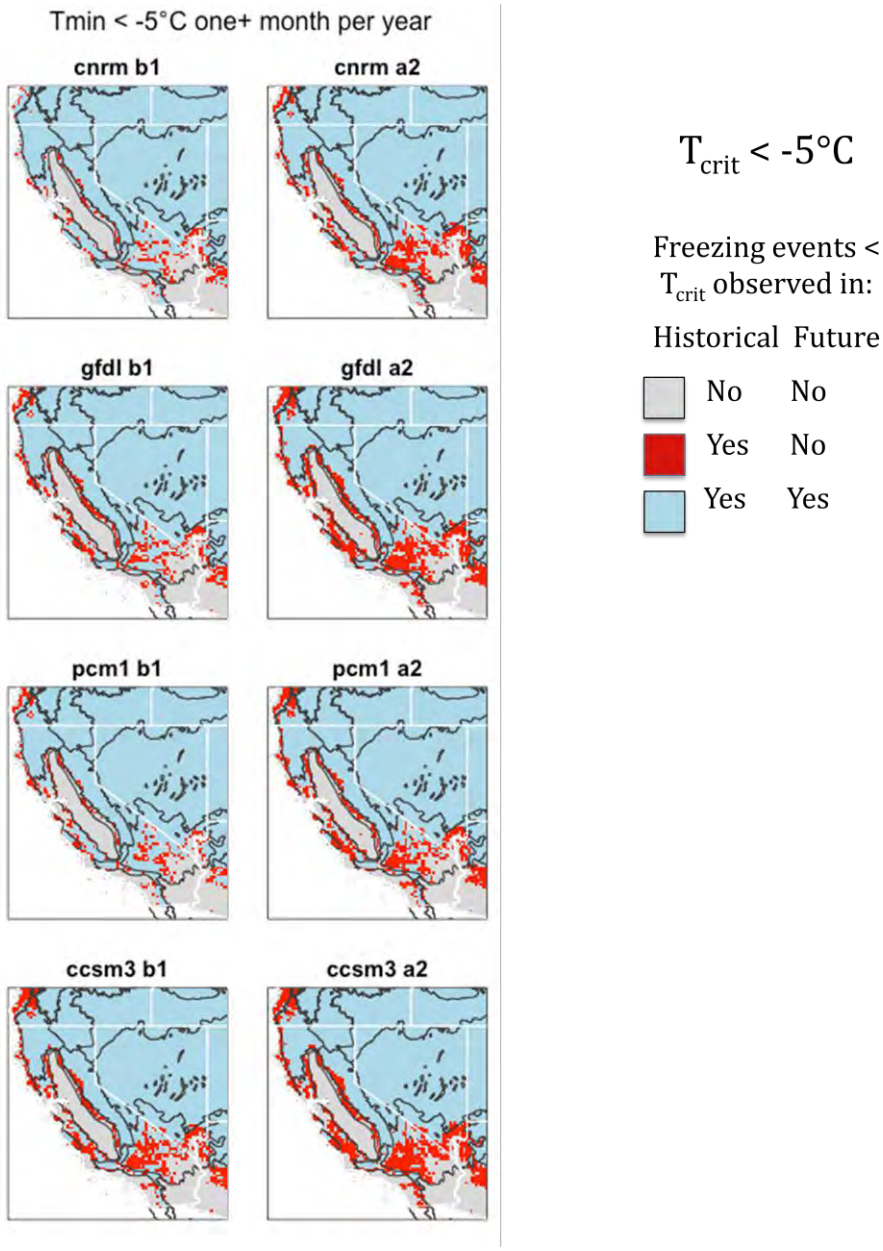

Figure A7. T_{crit} < -5°C Experienced at Least Once per Year, on Average, during the 30-year Period (see the full description above)

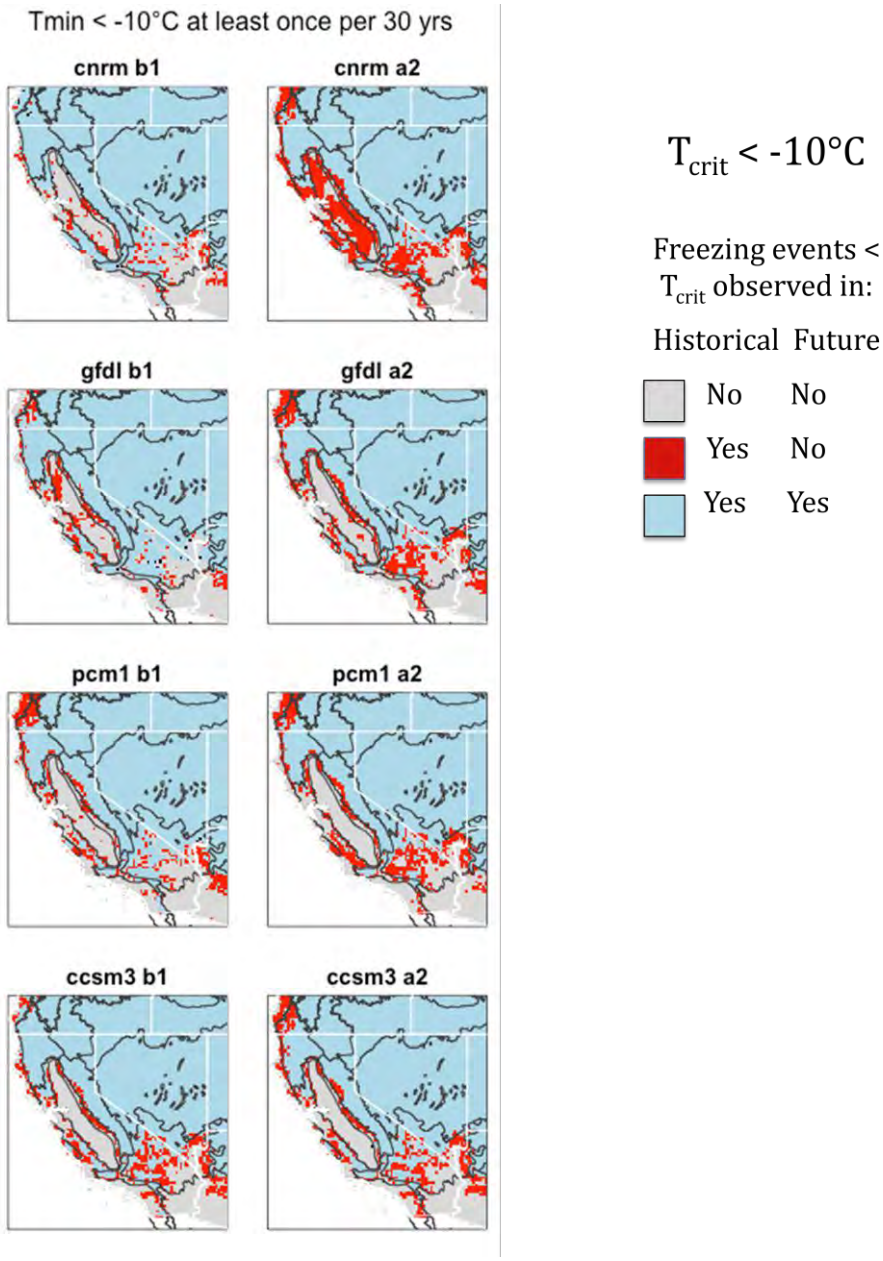

Figure A8. T_{crit} < -10°C Experienced at Least Once in the 30-year Period (see the full description above)

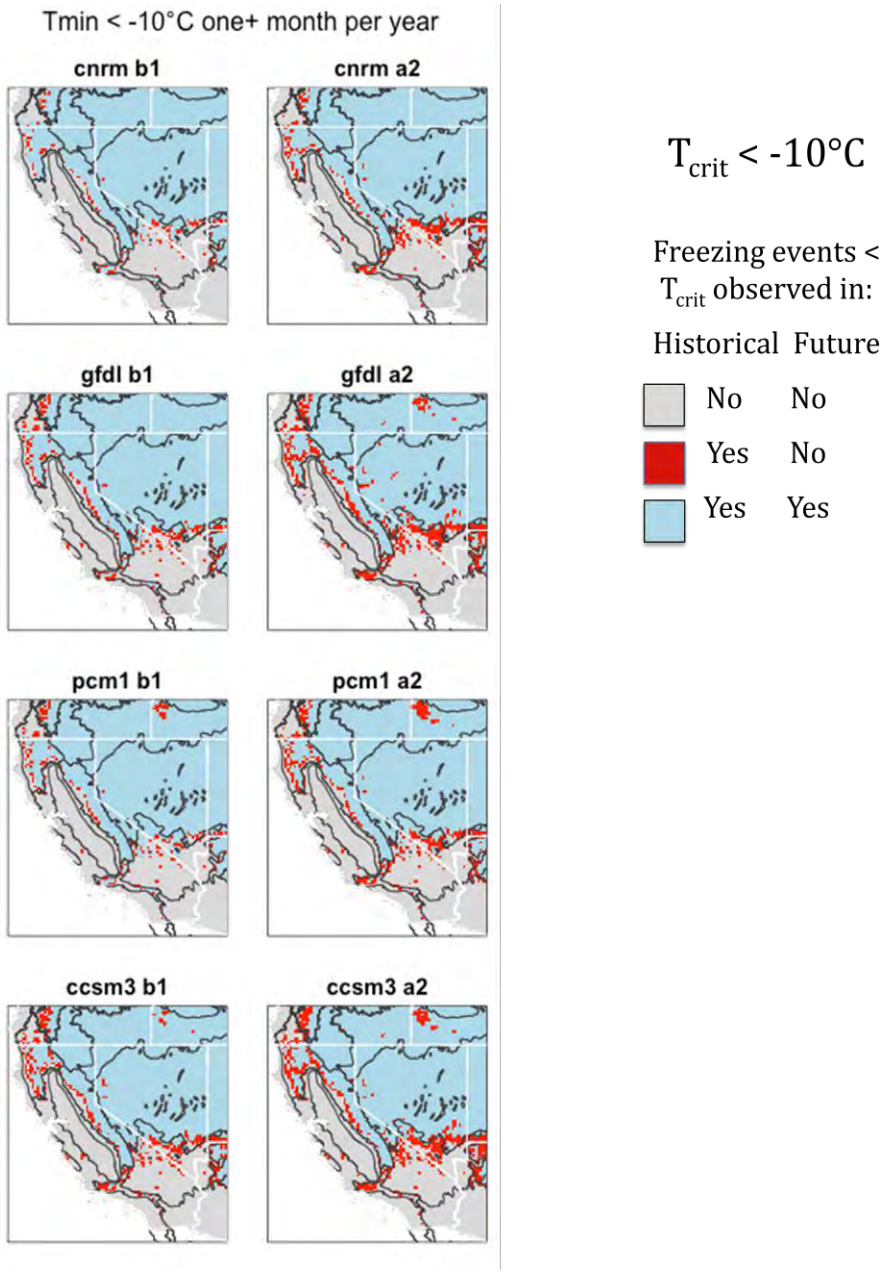

Figure A9. T_{crit} < -10°C Experienced at Least Once per Year, on Average, during the 30-year Period (see the full description above)

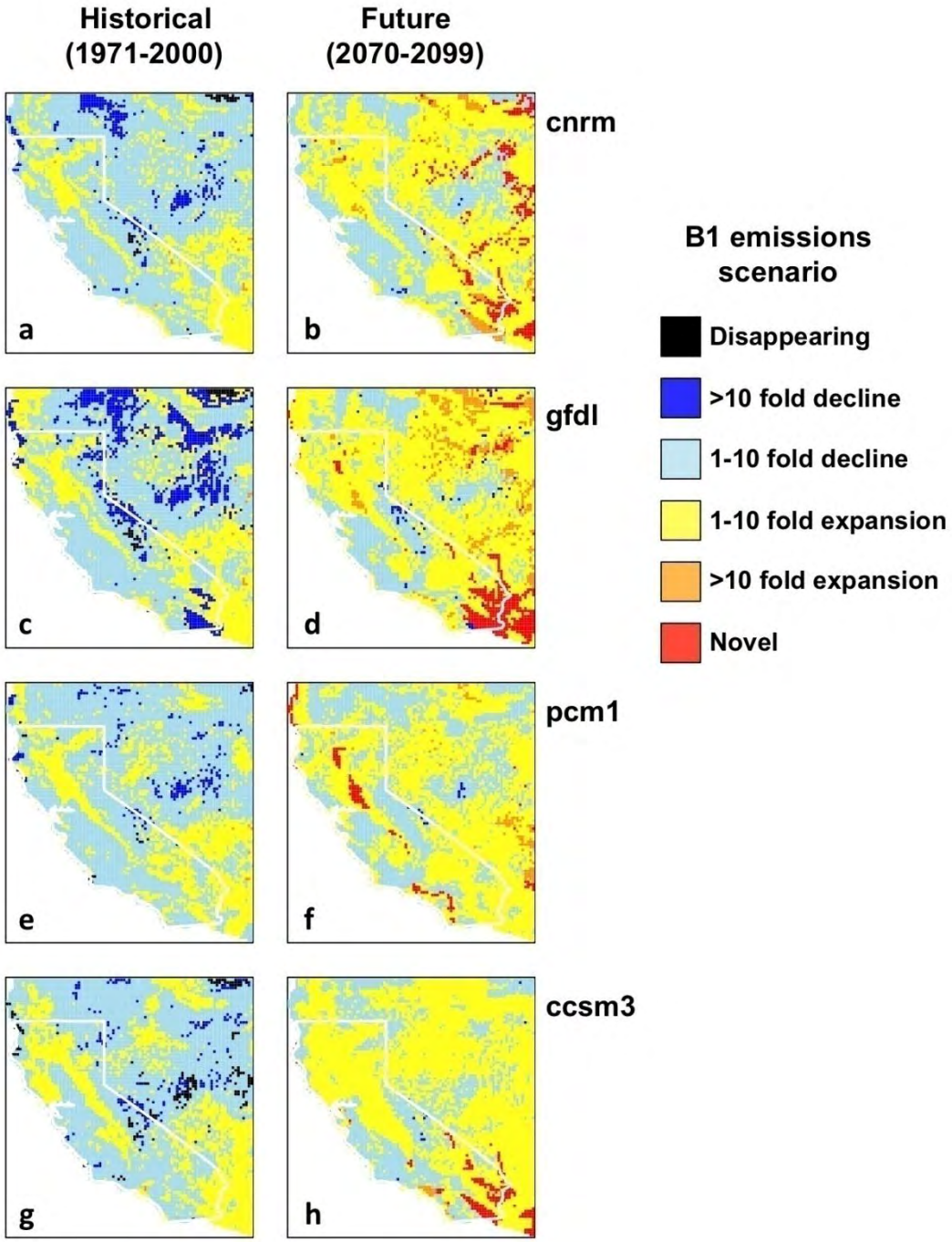

Figure A10. Novel, Disappearing, Expanding, and Shrinking Climates of California, Nevada, and Surrounding Areas, for the B1 Emissions Scenario. In each figure, left column shows the fate of current climates (1971–2000); right column shows status of projected future climates (2071–2100). Rows represent results for the CNRM, GFDL, PCM1, and CCSM3 general circulation models, downscaled for the 2008 California Climate Change Impacts Assessment Report. Colors: black = disappearing; dark blue = >10-fold reduction; light blue = 1- to 10-fold reduction; yellow = 1- to 10-fold expansion; orange = >10-fold expansion; red = novel climate. For example, in a row, the

areas mapped in yellow on left contain climates which will expand up to 10-fold in area, occupying the areas shown in yellow on the right.

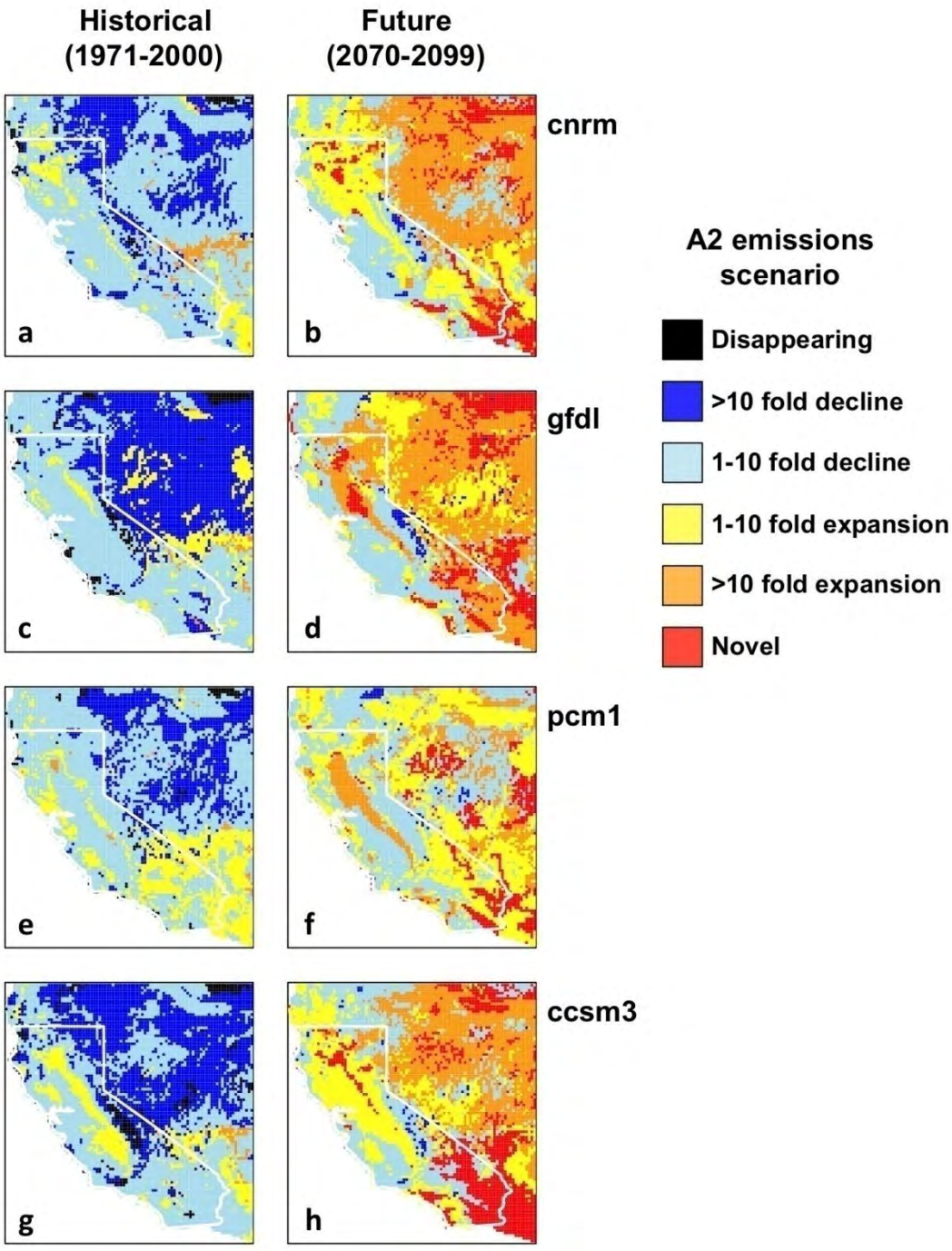

Figure A11. Same as Figure A10, for A2 Emissions Scenario